



Contents lists available at ScienceDirect

Arabian Journal of Chemistry

journal homepage: www.ksu.edu.sa

An integrated strategy for comprehensive characterization of chemical components in Qingqiao Kangdu granules by UHPLC-Q-Exactive-MS coupled with feature-based molecular networking

Kailin Li^{a,b,1}, Ping Wu^{c,1}, Sanyu Li^{c,1}, Yongliang Huang^c, Ling Wang^c, Yifan Chen^b, Yufeng Zou^b, Fang Yan^{a,*}, Wei Cai^{b,*}

^a Weifang Medical University, Weifang 261053, China

^b Hunan Province Key Laboratory for Antibody-based Drug and Intelligent Delivery System, School of Pharmaceutical Sciences, Hunan University of Medicine, Huaihua 418000, China

^c Hospital of Chengdu University of Traditional Chinese Medicine, Chengdu 610075, China

ARTICLE INFO

Keywords:

Qingqiao Kangdu granule
Characterization
UHPLC-Q-Exactive-MS
Feature-based molecular networking

ABSTRACT

Qingqiao Kangdu granule (QQKDG), a traditional Chinese medicine (TCM), has been used clinically to treat various viral diseases, including flu, mumps, and viral hepatitis, owing to its abundant bioactivities. Nevertheless, the chemical components of QQKDG have not been sufficiently elucidated; consequently, the development of standards for quality evaluation and complete understanding of the pharmacological mechanisms of action are hindered. Therefore, a systematic approach must be developed to efficiently discover novel compounds and advance pharmacological research. In this regard, this study proposed an integrated strategy for the comprehensive characterization of the chemical components in QQKDG by UHPLC-Q-Exactive-MS coupled with feature-based molecular networking (FBMN) to improve annotation accuracy and achieve visualization. First, the chromatographic and mass spectrum conditions were optimized to obtain good separation and abundant signal response. Subsequently, an in-house library was established by searching for relevant literature to improve annotation confidence. Finally, the raw data acquired under optimized conditions were uploaded to the FBMN to achieve component visualization by connecting precursor ions of the same color, in which compounds have similar structural features. Thus, a total of 231 compounds, including 89 flavonoids, 36 phenolic acids, 26 phenylethanoid glycosides, 23 coumarins, 17 chlorogenic acid derivatives, 14 terpenoids, 10 alkaloids, 10 lignans and 6 other compounds, were characterized, and numerous novel compounds with new structures were explored. Thus, this study provides a strategy for comprehensive characterization, which can also be applied to other TCMS.

1. Introduction

Currently, increasingly number of complex diseases that are difficult to control and cure using the conventional drug development philosophy of single-compound–single-target, whereby a drug with only one compound targets a specific protein to treat a particular disease, are surfacing (Hu and Sun, 2017; Wang et al., 2014). Since centuries, traditional Chinese medicines (TCMs) have been used extensively in China and other Asian countries to treat difficult miscellaneous diseases; they comprise several medicinal herbs mixed in a specific mass ratio

according to the rules of the monarch, minister, assistant, and guide (Pang et al., 2016; Wang et al., 2018). Recently, TCMS have received considerable attention in treating complicated and chronic diseases owing to their multicomponent, multipathway, and multitarget effects (Wang et al., 2020). For example, Yupingfeng San is a TCM formula that consists of three herbs, Huangqi, Fangfeng, and Baizhu in Chinese, which improve lung Qi, relieve pain, and enhance the spleen, owing to the antiimmunity, antiinflammatory, and gastrointestinal tract regulation effects based on the chemical components of flavonoids, chromones, and sesquiterpenoids in lung diseases (Zhang et al., 2015;

Peer review under responsibility of King Saud University.

* Corresponding authors.

E-mail addresses: yanfang303@163.com (F. Yan), 20120941161@bucm.edu.cn (W. Cai).

¹ These authors contributed equally to the study.

<https://doi.org/10.1016/j.arabjc.2023.105463>

Received 18 July 2023; Accepted 16 November 2023

Available online 18 November 2023

1878-5352/© 2023 The Authors. Published by Elsevier B.V. on behalf of King Saud University. This is an open access article under the CC BY-NC-ND license (<http://creativecommons.org/licenses/by-nc-nd/4.0/>).

Aravilli et al., 2017; Xu and Zhang, 2020; Yang et al., 2021). Several TCMS can be combined with Western medicines to relieve clinical symptoms and reduce toxicity and side effects, thereby improving the quality of life of patients (Xu and Chen, 2010).

Qingqiaokangdu granule (QQKDG), a TCM formula, was developed by the hospital affiliated with the Chengdu University of TCM according to the local climatic characteristics and features of resident crowd. This QQKDG is composed of fourteen herbs, namely *Lonicera japonica* (yinhuateng), *Forsythia suspensa* (lianqiao), *Pueraria montana* (fenge), *Angelicae dahuricae* (baizhi), *Artemisia caruifolia* (qinghao), *Radix Bupleuri* (chaihu), *Paridis Rhizoma* (chonglou), the dried root of *Isatis tinctoria* (banlangen), the dried rhizoma of *Iris tectorum* (chunshengan), *Taraxacum mongolicum* (pugongying), the dried leaves of *Isatis indigotica* (daqingye), *Pogostemon cablin* (guanghuoxiang), *Perillae Folium* (zisuye), and *Mentha canadensis* (bohe) (Xiong et al., 2014). Modern pharmacological research has demonstrated that QQKDG has the effects of clearing heat, detoxifying, relieving external heat, and reducing fever; thus, it has been extensively used in treating viral diseases, including flu, mumps, and viral hepatitis (Xia et al., 2016). Its efficacy and safety have been proven in double-blind randomized, controlled clinical trials (Xiong, 2015). Although QQKDG has remarkable efficacy on anemopyretic cold, it contains numerous unknown chemical compounds, owing to which, elucidating the therapeutic material basis and action mechanisms, and their globalization are both challenging. Xia et al. developed a method based on high-performance liquid chromatography (HPLC) switching wavelengths to simultaneously determine the content of seven constituents in QQKDG (Xia et al., 2016). Therefore, the chemical compounds in QQKDG must be determined, which can be useful for quality control and standardization.

Ultra-high-performance liquid chromatography (UHPLC) coupled with high-resolution mass spectrometry (HRMS) is a powerful analytical tool for identifying and characterizing the chemical compounds in TCMS owing to its strong separation ability and structure prediction (Fu et al., 2021; Gao et al., 2021). Computer-aided software, developed primarily for targeted screening based on known databases, has the advantage of complex data processing and has greatly promoted the characterization of chemical components in TCMS, such as waters UNIFI and thermo fisher compound discover (Chen et al., 2021). Global natural products social (GNPS, <https://gnps.ucsd.edu/>) molecular networking (MN) is an open-access knowledge platform for the rapid clustering and analysis of mass spectrometry data; it was developed to comprehensively characterize the chemical ingredients of TCMS according to MS/MS spectrum similarity and public databases (Zhang et al., 2021). In addition, MN was applied to speculate unannotated nodes by relating them to structural analogs of annotated compounds based on MS data and fragmentation pathways (Zhang et al., 2022). Feature-based molecular networking (FBMN), a novel data analysis tool in MN, has been employed to distinguish isomers, essentially providing several advantages in visualizing and clustering unknown compounds (Li et al., 2022). It is beneficial for rapidly identifying compounds in complex systems and discovering unknown components owing to their strong integration and classification abilities. Therefore, in this study, an integrated strategy was established to rapidly detect and characterize the chemical components of QQKDG using UHPLC-Q-Exactive-MS coupled with FBMN. This is the first systematic investigation of the chemical composition of QQKDG, and the results provide a comprehensive understanding of the material basis of QQKDG against anemopyretic colds. This strategy also provides an efficient method for identifying ingredients in TCM prescriptions.

2. Materials and methods

2.1. Materials and reagents

QQKDG were obtained from the Hospital of the Chengdu University of TCM (Chengdu, China; batch number: 20220210). A total of 42

reference standards, including 22 flavonoids, 7 phenylpropanoids, 5 organic acids, 3 coumarins, 1 lignan, 1 terpenoid, 1 alkaloid, 1 paraben, and 1 phenylethanoid glycoside, were characterized by ¹HNMR, ¹³C NMR, and MS spectral analyses, and the purities were above 98 % by HPLC analysis. Detailed information regarding the reference standards is provided in **Supplementary Table S1**. Chromatography-grade methanol and acetonitrile were purchased from Merck (Kenilworth, NJ, USA). Distilled water was obtained from Guangzhou Watson Food and Beverage Co., Ltd. (Guangzhou, China). LC-MS-grade formic acid was purchased from Fisher Scientific (Waltham, MA). All the other reagents were of analytical grade.

2.2. Sample preparation

QQKDG (5 g) was ultrasonically extracted with 70 % methanol (100 mL) for 1 h at room temperature. The extracting solution was concentrated at 50 °C using a rotary vacuum evaporator and water was removed using a freeze dryer to obtain the residue of QQKDG. Subsequently, the portion of QQKDG was dissolved in methanol and centrifuged at 12000 rpm for 20 min, and filtered through a 0.22- μ m millipore filter before LC-MS analysis.

The 42 reference standards were dissolved in methanol at an approximate concentration of 1 mg/mL. Each stock solution was mixed and diluted in methanol to obtain the standard mixture solution (approximately 20 μ g/mL). Subsequently, the mixed solution was centrifuged at 12000 rpm for 20 min, and the supernatant was stored at 4 °C before analysis.

2.3. Liquid chromatographic conditions

Chromatographic separation of the sample was performed using an Ultimate 3000 UHPLC system (Thermo Fisher Scientific, California, USA) equipped with a binary pump, autosampler, degasser, and column compartment. The separation of the QQKDG was performed on a Thermo Scientific Synchronis C18 (100 mm \times 2.1 mm, 1.7 μ m) at 45 °C. The mobile phase consisted of 0.1 % formic acid in water (A) and acetonitrile (B). The flow rate was 0.28 mL/min, and the gradient elution program was optimized as: 0–2 min, 5–10 % B; 2–5 min, 10–15 % B; 5–10 min, 15–20 % B; 10–12 min, 20–40 % B; 12–20 min, 40–55 % B; 20–25 min, 55–80 % B; 25–26 min, 80–5 % B; and 26–30 min, 5 % B. The injection volume was 2 μ L.

2.4. MS spectrometry conditions

Mass spectrometry was performed using a Q-Exactive Orbitrap MS (Thermo Fisher Scientific, Bremen, Germany) instrument equipped with a heated electrospray ionization source (HESI). Data acquisition progressed in both positive and negative ion modes through full-scan data-dependent MS/MS (full scan-ddMS²) with a mass range of m/z 100–1500. Mass spectrometry conditions were set as follows. The capillary voltage was set as 3.5 kV in the positive ion mode and 3.0 kV in the negative ion mode; the full mass resolution was set to 70000; the heater temperature and heated capillary temperature were 350 and 320 °C, respectively; the sheath gas and auxiliary gas flow rate were 30 and 10 arb, respectively; the S-lens radio frequency (RF) level was 50; and the ddMS² resolution was set to 17500. The stepped normalized collision energies (NCEs) of 30, 40, and 60 % were employed for fragmentation. Xcalibur 4.2 software (Thermo Fisher Scientific, California, USA) was used for data acquisition and analysis.

2.5. Feature-based molecular networking analysis

The UHPLC-Q-Exactive-MS raw data in positive and negative ionization modes were converted to mzXML format with MS conversion and then imported into MZmine (version 2.53) for chromatographic feature extraction. The MZmine filter parameters are listed in **Supplementary**

Table S2. Two files, the feature quantification table (.CSV file) with peak areas and MS² spectral summaries (.MGF file) with a representative MS² spectrum were exported from MZmine; subsequently, the MS² file MGF, feature quantification table, and original mzML were imported into the GNPS FBMN analysis website (<https://gnps-quickstart.ucsd.edu/featurebasednetworking>) and visualized using Cytoscape 3.9.1. The molecular networking parameters included a precursor ion mass tolerance of 0.02 Da, minimum matched peaks > 6, cosine score of > 0.7, and library search matched peaks > 3.

3. Results and discussion

3.1. Integrated strategy for data analysis

QQKDG is composed of 14 herbs containing tens of thousands of compounds. Thus, herein, an effective strategy was established to comprehensively and accurately characterize the chemical constituents of QQKDG in Fig. 1. This strategy comprises three steps. First, to achieve good separation and abundant signal response, the proportion and variety of mobile phases, including acetonitrile-aqueous, methanol-aqueous, acetonitrile-aqueous with 0.1 % formic acid, and methanol-aqueous with 0.1 % formic acid, were optimized to obtain better chromatographic conditions. Thus, the mobile phases consisted of acetonitrile-aqueous with 0.1 % formic acid, which could be considered as the most optimized separation condition, and the proportion was in “2.3 Liquid chromatographic conditions.” Second, information regarding the compound names, molecular formulae, and exact MS/MS fragment ions of the chemical components derived from the 14 herbs of QQKDG were obtained from PubChem (<https://pubchem.ncbi.nlm.nih.gov>), CNKI (<https://www.cnki.net>), Web of Science (<https://www.webofknowledge.com>), and Google Scholar (<https://scholar.google.com/>) to develop an in-house library of QQKDG. The unknown compounds were identified by comparing the quasi-molecular ion and MS² fragment ions using an in-house library, and the fragmentation patterns were summarized based on existing standards. Third, GNPS were used to detect and identify unknown compounds based on fragment similarity. Raw data, including MS and MS/MS spectra, were converted into mzXML format and uploaded to mzmime software for data preprocessing; subsequently, the files of the quantification table and MS² spectral summary were imported into the GNPS-FBMN platform. In addition, the MS² fragment ions were matched with the GNPS database for a fast and accurate analysis. Unannotated compounds were identified according to the MS/MS spectral relevance between the annotated compounds and in-house library.

3.2. Characterization of chemical constituents in QQKDG by UHPLC-Q-Exactive-MS based on FBMN

In this study, 231 compounds were detected, of which 42 compounds were precisely identified and 189 compounds were putatively identified using the integrated strategy; these compounds included 89 flavonoids, 36 phenolic acids, 25 phenylethanoid glycosides, 23 coumarins, 17 chlorogenic acid derivatives, 14 terpenoids, 10 alkaloids, 10 lignans, and 7 others. Detailed information of components, including peak number, retention time (Rt), accurate molecular ions, formulas, mass errors (within ± 5 ppm), fragment ions and compound names, are presented in Table 1 and Supplementary Table S3. High-resolution extracted ion chromatograms (HREICs) of QQKDG in both positive and negative ion modes are shown in Fig. 2. In addition, the raw data in the two ion modes were processed using FBMN, an advanced processing method for distinguishing isomers with similar MS² spectra (Qu et al., 2023). Compounds of the same type could be clustered together and annotated by matching the MS/MS fragment ions of the FBMN database. Therefore, a comprehensive FBMN of QQKDG based on MS/MS spectral similarity was obtained, as shown in Supplementary Fig. S1. The molecular map contained a total of 2867 precursor ions, including 354 clusters (nodes, ≥ 2) and 3580 edges in negative mode, and a total of 2936 precursor ions, including 298 clusters (nodes, ≥ 2) and 4282 edges in positive mode. More detailed information is available on the open website (<https://gnps.ucsd.edu/ProteoSAFe/status.jsp?task=445f9d16f4774ce0a7be99730bc6dcf1> in the negative mode; <https://gnps.ucsd.edu/ProteoSAFe/status.jsp?task=c4b076f753b944dd94b8101de8abafe0> in the positive mode).

3.2.1. Identification of flavonoids

Flavonoids are hydroxylated phenolic substances that exist as aglycones, glycosides or methylated derivatives as the secondary metabolites of plants in natural world (Harborne, 2013). The flavonoid could be subdivided into different subclasses according to the location of the B ring connection, the degree of unsaturation of the C ring and oxidation including isoflavones, flavones, flavonols, flavanones, dihydrochalcones, etc. (Corradini et al., 2011; Karak, 2019; Dias et al., 2021). In this study, a total of 89 flavonoids including 37 isoflavones, 29 flavones, 16 flavonols, 3 flavanones, 3 chromones, 1 dihydrochalcone, were detected and characterized in QQKDG based on FBMN and in-house library (Fig. 3). The identified isoflavones were derived primarily from *Belamcanda chinensis* and *Puerariae lobatae*, which are also a rich source of isoflavones and have an intense effect of anti-bacterial, anti-inflammatory, relieving pain (Wozniak et al., 2010; Choi et al., 2016). Reportedly, glycosyl group was easily substituted at the 7 or 4' position of aglycones; consequently, the

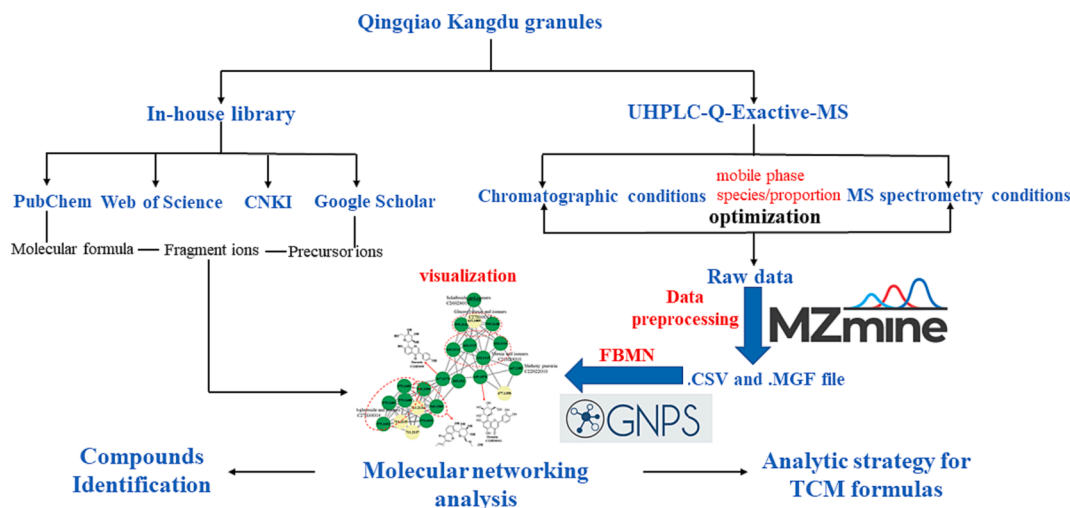


Fig. 1. An integrated strategy for chemical characterization of QQKDG extract.

Table 1 (continued)

peak	t _R	Theoretical Mass m/z	Experimental Mass m/z	Error (ppm)	Formula	Identification	peak	t _R	Theoretical Mass m/z	Experimental Mass m/z	Error (ppm)	Formula	Identification
30	5.21	407.09837	407.09793	-1.30	C ₁₉ H ₂₀ O ₁₀	Iriflophenone-2-O-β-glucoside	146	12.54	623.19814	623.19757	-0.92	C ₂₉ H ₃₆ O ₁₅	Forsythoside I
31	5.33	375.12967	375.12924	-1.15	C ₁₆ H ₂₄ O ₁₀	Adoxosidic acid	147	12.55	357.13436	357.13370	-1.85	C ₂₀ H ₂₂ O ₆	Epipinoresinol
32	5.40	355.10345	355.10336	-0.27	C ₁₆ H ₂₀ O ₉	ferulic acid-O-glucoside	148	12.55	519.18718	519.18646	-1.40	C ₂₆ H ₃₂ O ₁₁	Pinoresinol-O-glucoside
33	5.44	337.09289	337.09280	-0.27	C ₁₆ H ₁₈ O ₈	p-coumaroylquinic acid	149	12.56	477.10384	477.10342	-0.90	C ₂₂ H ₂₂ O ₁₂	Isorhamnetin-3-O-glucoside
34	5.48	709.19853	709.19836	-0.25	C ₃₂ H ₃₈ O ₁₈	Mirificin-4'-O-glucoside	150	12.56	538.22828 [M + NH ₄] ⁺	538.22638	-3.54	C ₂₆ H ₃₂ O ₁₁	Matairesinol-4-O-D-glucopyranoside
35	5.51	341.08781	341.08771	-0.28	C ₁₅ H ₁₆ O ₉	caffeic acid-O-glucoside	151	12.57	247.09648	247.09549	-4.03	C ₁₄ H ₁₄ O ₄	Columbianetin
36	5.60	295.04594	295.04562	-1.09	C ₁₃ H ₁₂ O ₈	coumaroyl-tartaric acid	152	12.60	607.20322	607.20325	0.04	C ₂₉ H ₃₆ O ₁₄	Forsythenside K
37	5.62	389.10893	389.10855	-0.99	C ₁₆ H ₂₂ O ₁₁	secologanoside	153	12.68	623.16175	623.16022	-2.47	C ₂₈ H ₃₂ O ₁₆	Isorhamnetin-3-O-β-D-rutinoside
38	5.74	327.13393	327.13245	-7.89	C ₁₈ H ₁₈ N ₂ O ₄	isaindigodione isomer	154	12.72	433.11402	433.11383	-0.44	C ₂₁ H ₂₂ O ₁₀	Naringenin-7-O-glucoside
39	5.74	579.17083	579.16858	-3.89	C ₂₇ H ₃₀ O ₁₄	Daidzein-4,7-O-glucoside	155	12.74	491.11949	491.11890	-1.22	C ₂₃ H ₂₄ O ₁₂	Iristectorin B
40*	5.79	353.08780355.10235	353.08734	-1.32	C ₁₆ H ₁₈ O ₉	Chlorogenic acid	156	12.81	349.08636	349.08618	-0.53	C ₁₆ H ₁₈ N ₂ O ₅ S	Indole-3-acetonitrile-2-S-β-D-glucopyranoside
41	5.82	373.11402	373.11349	-1.42	C ₁₅ H ₂₀ O ₈	Androsin	157	12.90	503.17701	503.17767	1.30	C ₂₀ H ₂₈ O ₁₁	Hyuganoside IV
42	5.98	253.07176	253.07141	-1.39	C ₁₂ H ₁₄ O ₆	hwanggeumchal B isomer 1	158	12.95	477.10384 479.11840	477.10330	-1.15	C ₂₂ H ₂₂ O ₁₂	Isorhamnetin-7-O-glucoside
43*	6.02	353.08780355.10235	353.08737355.10068	-1.23-4.72	C ₁₆ H ₁₈ O ₉	Cryptochlorogenic acid	159	12.95	507.11441	507.11389	-1.03	C ₂₂ H ₂₂ O ₁₁	Isotectorigenin-7-O-β-D-glucoside isomer 2
44	6.03	355.10235	355.10068	-4.73	C ₁₆ H ₁₈ O ₉	Scopolin	160	12.98	445.07763447.09218	445.07724447.09067	-0.89 -3.39	C ₂₁ H ₁₈ O ₁₁	Apigenin-7-O-glucuronide
45	6.03	507.17192	507.17133	-1.18	C ₂₁ H ₃₂ O ₁₄	secologanoside A	161	12.99	717.14610	717.14618	0.10	C ₃₆ H ₃₀ O ₁₆	Salvianolic acid B
46	6.05	373.11402	373.11356	-1.23	C ₁₆ H ₂₂ O ₁₀	Swertiamarin	162	13.04	515.11949517.13405	515.11890517.13239	-1.16-3.21	C ₂₅ H ₂₄ O ₁₂	Isochlorogenic acid C
47	6.26	367.10345	367.10318	-0.75	C ₁₇ H ₂₀ O ₉	Feruloylquinic acid	163	13.10	719.16175	719.16113	-0.87	C ₃₆ H ₃₂ O ₁₆	Sagerinic acid
48	6.40	177.01933	177.01837	-5.43	C ₉ H ₆ O ₄	Daphnetin	164	13.10	359.07724	359.07681	-1.20	C ₁₈ H ₁₆ O ₈	Rosmarinic acid
49*	6.50	179.03498	179.03394	-5.82	C ₉ H ₈ O ₄	Caffeic acid	165	13.14	491.11949	491.11890	-1.22	C ₂₃ H ₂₄ O ₁₂	Iristectorin A
50	6.67	355.10345	355.10355	0.27	C ₁₆ H ₂₀ O ₉	ferulic acid-O-glucoside	166	13.20	521.13006523.14461	521.12952523.14252	-1.04-4.00	C ₂₄ H ₂₆ O ₁₃	Iridin
51	6.73	593.15119	593.15100	-0.33-3.75	C ₂₇ H ₃₀ O ₁₅	Glucosylvitexin	167	13.21	267.07641	267.07529	-4.23	C ₁₅ H ₁₀ O ₃ N ₂	3-(2'-carboxyPhenyl)-4-(3H)-quinazolinone
52	6.79	627.15557	627.15350	-3.31	C ₂₇ H ₃₀ O ₁₇		168	13.21	435.12967	435.12897	-1.61	C ₂₁ H ₂₄ O ₁₀	Phlorizin
53	6.84	579.17083	579.16876	-3.58	C ₂₇ H ₃₀ O ₁₄	6"-O-α-D-glucopyranosylpuerarin	169	13.24	459.12857	459.12683	-3.80	C ₂₃ H ₂₂ O ₁₀	6"-O-Acetyl daidzin
54	6.89	481.09876	481.09842	-0.72	C ₂₁ H ₂₂ O ₁₃	gallic acid-3-methyl ether-4-O-protocatechuoylglucoside	170	13.26	621.18249	621.18250	0.01	C ₂₉ H ₃₄ O ₁₅	Suspensaside A
55	6.92	579.17083	579.16852	-3.99	C ₂₇ H ₃₀ O ₁₄	3'-Methoxypuerarin-O-apioside	171	13.34	519.18718	519.18701	-0.34	C ₂₆ H ₃₂ O ₁₁	Matairesinoside
56*	6.95	342.16998	342.16867	-3.84	C ₂₀ H ₂₄ O ₄ N	Magnoflorine	172	13.39	473.14532	473.14520	-0.25	C ₂₄ H ₂₆ O ₁₀	Sophoraside A
57	6.96	253.07176	253.07141	-1.39	C ₁₂ H ₁₄ O ₆	hwanggeumchal B isomer 2	173	13.39	519.15079	519.15100	0.39	C ₂₅ H ₂₈ O ₁₂	Pueroside C
58*	7.06	417.11800	417.11606	-4.67	C ₂₁ H ₂₀ O ₉	Puerarin	174	13.40	373.12927	373.12967	1.06	C ₂₀ H ₂₂ O ₇	(+)-1-Hydroxylpinoresinol
59	7.12	639.19305	639.19287	-0.29	C ₂₉ H ₃₆ O ₁₆	R-suspensaside	175	13.61	315.05102	315.05084	-0.59	C ₁₆ H ₁₂ O ₇	Irilin D
60	7.13	707.25215	707.24933	-4.00	C ₃₂ H ₄₄ O ₁₆	Lariciresinol-4,4'-O-β-D-diglucoside	176	13.62	431.13365	431.13217	-3.45	C ₂₂ H ₂₂ O ₉	Ononin

(continued on next page)

Table 1 (continued)

peak	t _R	Theoretical Mass m/z	Experimental Mass m/z	Error (ppm)	Formula	Identification	peak	t _R	Theoretical Mass m/z	Experimental Mass m/z	Error (ppm)	Formula	Identification
61	7.14	729.26113	729.26111	-0.04	C ₃₂ H ₄₄ O ₁₆	Clemastanin B	177	13.68	467.21339	467.21368	0.60	C ₂₀ H ₃₆ O ₁₂	N-octanoylsucrose
62	7.16	387.16605	387.16574	-0.82	C ₁₈ H ₂₈ O ₉	Jasmonic acid-5'-O-glucoside	178	13.81	239.08150	239.08054	-4.03	C ₁₄ H ₁₀ O ₂ N ₂	3-(2'-Hydroxyphenyl)-4-(3H)-quinazolinone
63	7.28	639.19305	639.19318	0.19	C ₂₉ H ₃₆ O ₁₆	isocampneoside II	179	13.83	431.13365	431.13223	-3.31	C ₂₂ H ₂₂ O ₉	Isoononin
64*	7.33	403.12458	403.12405	-1.33	C ₁₆ H ₂₂ O ₉	Sweroside	180	13.87	283.15509	283.15482	-0.98	C ₁₅ H ₂₄ O ₅	Dihydroartemisinin
65	7.35	435.15079	435.15027	1.30	C ₁₇ H ₂₆ O ₁₀	Loganin	181	13.90	255.06518	255.06404	-4.49	C ₁₅ H ₁₀ O ₄	Daidzein
66	7.39	337.09289	337.09283	-0.18	C ₁₆ H ₁₈ O ₈	p-Coumaroylquinic acid	182	13.90	579.20831	579.20770	-1.06	C ₂₇ H ₃₄ O ₁₁	Forsythin
67	7.46	593.15119	593.15100	-0.33-3.53	C ₂₇ H ₃₀ O ₁₅	Vicenin II	183	13.96	203.03388	203.03311	-3.82	C ₁₁ H ₆ O ₄	Xanthotoxol
68	7.51	639.19305	639.19293	-0.20	C ₂₉ H ₃₆ O ₁₆	S-suspensaside	184	13.96	287.09140	287.09018	-4.25	C ₁₆ H ₁₄ O ₅	Oxypeucedanin
69*	7.56	547.14571	547.14539	-0.59-4.09	C ₂₆ H ₂₈ O ₁₃	Puerarin apioside	185	13.96	305.10196	305.10077	-3.92	C ₁₆ H ₁₆ O ₆	Prangenin hydrate
70*	7.63	515.11949517.13405	515.11902517.13257	-0.93-2.86	C ₂₅ H ₂₄ O ₁₂	1,3-Dicaffeoylquinic acid	186	13.96	504.18751	504.18851	1.97	C ₂₅ H ₃₁ NO ₁₀	L-Phenylalaninosecologanin B
71	7.67	653.17232	653.17212	-0.31-3.04	C ₂₉ H ₃₄ O ₁₇	Iristectorin B-4'-O-glucoside	187	14.03	677.15119	677.15070	-0.73	C ₃₄ H ₃₀ O ₁₅	3, 4, 5-O-tricaffeoylquinic acid
72	8.01	637.10463	637.10455	-0.14	C ₂₇ H ₂₆ O ₁₈	Scutellarein-7-O-diglucuronide	188	14.08	319.11761	319.11630	-4.12	C ₁₇ H ₁₈ O ₆	3'-O-Acetylhamaudol
73	8.09	639.19305	639.19312	0.10	C ₂₉ H ₃₆ O ₁₆	Lugrandoside	189	14.09	653.17232	653.17151	-1.24	C ₂₉ H ₃₄ O ₁₇	Iristectorigenin B-7-O-β-glucosyl(1 → 6)-glucoside isomer
74	8.30	239.09249	239.09195	-2.29	C ₁₂ H ₁₆ O ₅	3,4'-Dihydroxy-3'-methoxy-benzenepentanoic acid	190	14.20	285.04046	285.04013	-1.16	C ₁₅ H ₁₀ O ₆	Luteolin
75	8.30	579.17083	579.16882	-3.47	C ₂₇ H ₃₀ O ₁₄	3'-Methoxydaidzin-O-apioside	191	14.21	301.03537	301.03500	-1.25	C ₁₅ H ₁₀ O ₇	Quercetin
76	8.31	593.15119	593.15094	-0.43-3.85	C ₂₇ H ₃₀ O ₁₅	Glucosyl-vitexin	192	14.36	305.10196	305.10083	-3.72	C ₁₆ H ₁₆ O ₆	Oxypeucedan hydrate
77	8.31	639.19305	639.19263	-0.67	C ₂₉ H ₃₆ O ₁₆	R-campneoside II	193	14.54	207.06628	207.05037	-3.17	C ₁₁ H ₁₂ O ₄	Ethyl caffeate
78	8.37	403.12458	403.12405	-1.33	C ₁₇ H ₂₄ O ₁₁	Secoxyloganin	194	14.57	335.11252	335.11087	-4.95	C ₁₇ H ₁₈ O ₇	Byakangelicin
79	8.37	563.14062	563.14020	-0.76	C ₂₆ H ₂₈ O ₁₄	Schaftoside	195	14.57	317.10196	317.10046	-4.75	C ₁₇ H ₁₆ O ₆	Byakangelicol
80	8.37	637.10463	637.10419	-0.70	C ₂₇ H ₂₆ O ₁₈	Luteolin-7-O-diglucuronide	196	14.93	271.06119	271.06100	-0.73	C ₁₅ H ₁₂ O ₅	Naringenin
81	8.39	367.10345	367.10297	-1.32-4.19	C ₁₇ H ₂₀ O ₉	Feruloylquinic acid	197	15.02	269.04554	269.04532	-0.84	C ₁₅ H ₁₀ O ₅	Apigenin
82	8.45	639.19305	639.19348	0.66	C ₂₉ H ₃₆ O ₁₆	S-campneoside II	198	15.05	387.14492	387.14471	-0.56	C ₂₁ H ₂₄ O ₇	5'-O-caffeoyl-jasmonic acid
83	8.66	449.14532	449.14478	-1.20	C ₂₂ H ₂₆ O ₁₀	Forsythenside F	199	15.22	285.04046	285.04010	-1.27	C ₁₅ H ₁₀ O ₆	Kaempferol
84	8.69	417.11800	417.11612	-4.53	C ₂₁ H ₂₀ O ₉	Daidzin	200	15.23	299.05611	299.05566	-1.51	C ₁₆ H ₁₂ O ₆	Tectorigenin
85	8.78	639.19305	639.19275	-0.48	C ₂₉ H ₃₆ O ₁₆	Isolugrandoside	201	15.50	315.05102	315.05084	-0.59	C ₁₆ H ₁₂ O ₇	Isorhamnetin
86	8.81	563.14062	563.14038	-0.44-3.82	C ₂₆ H ₂₈ O ₁₄	Vicenin III	202	15.56	329.06667	329.06635	-0.99	C ₁₇ H ₁₄ O ₇	Iristectorigenin A
87*	8.92	447.09328449.10783	447.09293449.10663	-0.79	C ₂₁ H ₂₀ O ₁₁	Orientin	203	15.62	277.10705	277.10587	-4.26	C ₁₅ H ₁₆ O ₅	3'(R)-+Hamadul
88	9.07	187.08658	187.08591	-3.63	C ₁₁ H ₁₀ N ₂ O	Deoxyvasicinone	204	15.65	217.04953	217.04863	-4.17	C ₁₂ H ₈ O ₄	Bergapten
89	9.16	447.09328449.10783	447.09290449.10660	-0.86-2.75	C ₂₁ H ₂₀ O ₁₁	Homoorientin	205	15.78	359.07724	359.07690	-0.95	C ₁₈ H ₁₆ O ₈	Irigenin

(continued on next page)

Table 1 (continued)

peak	t _R	Theoretical Mass m/z	Experimental Mass m/z	Error (ppm)	Formula	Identification	peak	t _R	Theoretical Mass m/z	Experimental Mass m/z	Error (ppm)	Formula	Identification
90	9.17	477.06746	477.06732	-0.30	C ₂₁ H ₁₈ O ₁₃	Quercetin-3-O-β-D-Glucuronide	206	15.79	329.06667	329.06647	-0.63	C ₁₇ H ₁₄ O ₇	Iristectorigenin B
91	9.26	535.18209	535.18195	-0.28	C ₂₆ H ₃₂ O ₁₂	(+)-Hydroxylpinoselinol-4'-O-glucopyranoside	207	16.06	359.07724	359.07700	-0.67	C ₁₈ H ₁₆ O ₈	Sudachitin
92	9.32	431.09837433.11292	431.09790433.11136	-1.09-3.60	C ₂₁ H ₂₀ O ₁₀	Vitexin	208	16.43	279.07641	279.07541	-3.62	C ₁₆ H ₁₀ N ₂ O ₃	Hydroxy lindirubin
93	9.36	447.09328449.10783	447.09290449.10620	-0.86-3.647	C ₂₁ H ₂₀ O ₁₁	Kaempferol-7-O-β-D-glucopyranoside	209	16.44	267.06628	267.06580	-1.81	C ₁₆ H ₁₂ O ₄	Formononetin
94	9.38	609.18249	609.18225	-0.40	C ₂₈ H ₃₄ O ₁₅	Forsythoside J	210	16.60	217.04953	217.04887	-3.07	C ₁₂ H ₈ O ₄	Xanthotoxin
95	9.45	579.17192	579.17163	-0.52	C ₂₇ H ₃₂ O ₁₄	Naringin	211	16.68	247.06009	247.05922	-3.562	C ₁₃ H ₁₀ O ₅	Isopimpinellin
96	9.47	477.10384 479.11840	477.10364	-0.44	C ₂₂ H ₂₂ O ₁₂	3'-Hydroxytectoridin	212	17.18	327.05102	327.05075	-0.84	C ₁₇ H ₁₂ O ₇	Iriflogenin
97	9.51	563.14062 565.15518	563.14020	-0.76	C ₂₆ H ₂₈ O ₁₄	Isoschaftoside	213	17.36	249.06585	249.06487	-3.95	C ₁₅ H ₈ N ₂ O ₂	Tryptanthrin
98	9.64	639.19305	639.19299	-0.11	C ₂₉ H ₃₆ O ₁₆	Plantamajoside isomer	214	17.39	825.46419	825.46454	0.42	C ₄₂ H ₆₈ O ₁₃	Saikosaponin A
99*	9.68	447.09328449.10783	447.09293449.10641	-0.79-3.17	C ₂₁ H ₂₀ O ₁₁	Luteolin-7-O-glucoside	215	17.93	233.04444	233.04349	-4.12	C ₁₂ H ₈ O ₅	5-Methoxy-8-hydroxypsoralen
100	9.69	607.20213	607.20044	-2.79	C ₂₉ H ₃₄ O ₁₄	Pueroside A	216	18.07	359.07614	359.07474	-3.91	C ₁₈ H ₁₄ O ₈	Dichotomitin
101	9.74	187.03897	187.03841	-3.00	C ₁₁ H ₆ O ₃	Isopsoralen	217	18.30	191.10665	191.10577	-4.64	C ₁₂ H ₁₄ O ₂	Ligustilide
102	9.80	473.07254	473.07196	-1.25	C ₂₂ H ₁₈ O ₁₂	Cichoric acid	218	18.37	373.09289	373.09253	-0.97	C ₁₉ H ₁₈ O ₈	Junipegenin C
103	9.83	623.16175 625.17631	623.16113 625.17365	-1.01-4.25	C ₂₈ H ₃₂ O ₁₆	Tectorigenin-7-O-β-glucosyl (1 → 6) glucoside	219	18.56	283.06119	283.06097	-0.80	C ₁₆ H ₁₂ O ₅	Oroxilin A
104	9.86	187.03897	187.03812	-4.55	C ₁₁ H ₆ O ₃	Psoralen	220	18.87	283.06119	283.06094	-0.91	C ₁₆ H ₁₂ O ₅	Genkwanin
105	9.91	609.18249	609.18231	-0.30	C ₂₈ H ₃₄ O ₁₅	Calceolarioside C	221	18.92	249.14852	249.14734	-4.74	C ₁₅ H ₂₀ O ₃	Arteannuin
106	10.02	477.14023	477.13956	-1.41	C ₂₃ H ₂₆ O ₁₁	Calceolarioside A	222	19.19	263.08150	263.08047	-3.93	C ₁₆ H ₁₀ N ₂ O ₂	Indigo
107	10.04	193.04953	193.04874	-4.12	C ₁₀ H ₈ O ₄	Scopoletin	223	19.74	867.47475	867.47522	0.53	C ₄₄ H ₇₀ O ₁₄	AcetylSaikosaponin
108	10.05	623.19814	623.19769	-0.73	C ₂₉ H ₃₆ O ₁₅	Forsythoside H	224	19.91	359.11252	359.11115	-3.84	C ₁₉ H ₁₈ O ₇	5-Hydroxy-3',4',6',7-tetramethoxyFlavone
109	10.08	417.11800	417.11609	-4.60	C ₂₁ H ₂₀ O ₉	Puerarin isomer	225	20.12	263.08150	263.08035	-4.39	C ₁₆ H ₁₀ N ₂ O ₂	Indirubin
110	10.17	609.18249	609.18243	-0.10	C ₂₈ H ₃₄ O ₁₅	Calceolarioside C	226	20.20	345.09687	345.09543	-4.20	C ₁₈ H ₁₆ O ₇	Penduletin
111	10.25	417.11800	417.11636	-3.95	C ₂₁ H ₂₀ O ₉	Daidzein 4'-O-glucoside	227	21.08	389.12309	389.12155	-3.97	C ₂₀ H ₂₀ O ₈	Artemetin
112	10.48	755.24040	755.23975	-0.86	C ₃₄ H ₄₄ O ₁₉	Forsythoside B	228	21.38	271.09648	271.09537	-4.12	C ₁₆ H ₁₄ O ₄	Isoimperatorin
113	10.49	609.14610	609.14575	-0.59	C ₂₇ H ₃₀ O ₁₆	Rutin	229	22.42	301.10705	301.10580	-4.15	C ₁₇ H ₁₆ O ₅	Cnidilin
114	10.62	463.08819465.10275	463.08807465.10141	-0.28-2.88	C ₂₁ H ₂₀ O ₁₂	Hyperoside	230	23.04	359.11252	359.11090	-4.54	C ₁₉ H ₁₈ O ₇	Corymbosin
115	10.74	431.09837433.11292	431.09784433.11111	-1.23-4.18	C ₂₁ H ₂₀ O ₁₀	Isovitexin	231	23.28	223.09758	223.09694	-2.88	C ₁₂ H ₁₆ O ₄	Pogostone
116	10.80	223.06009	223.05899	-4.98	C ₁₁ H ₁₀ O ₅	Saikochromone A							

* Compared with standard compounds.

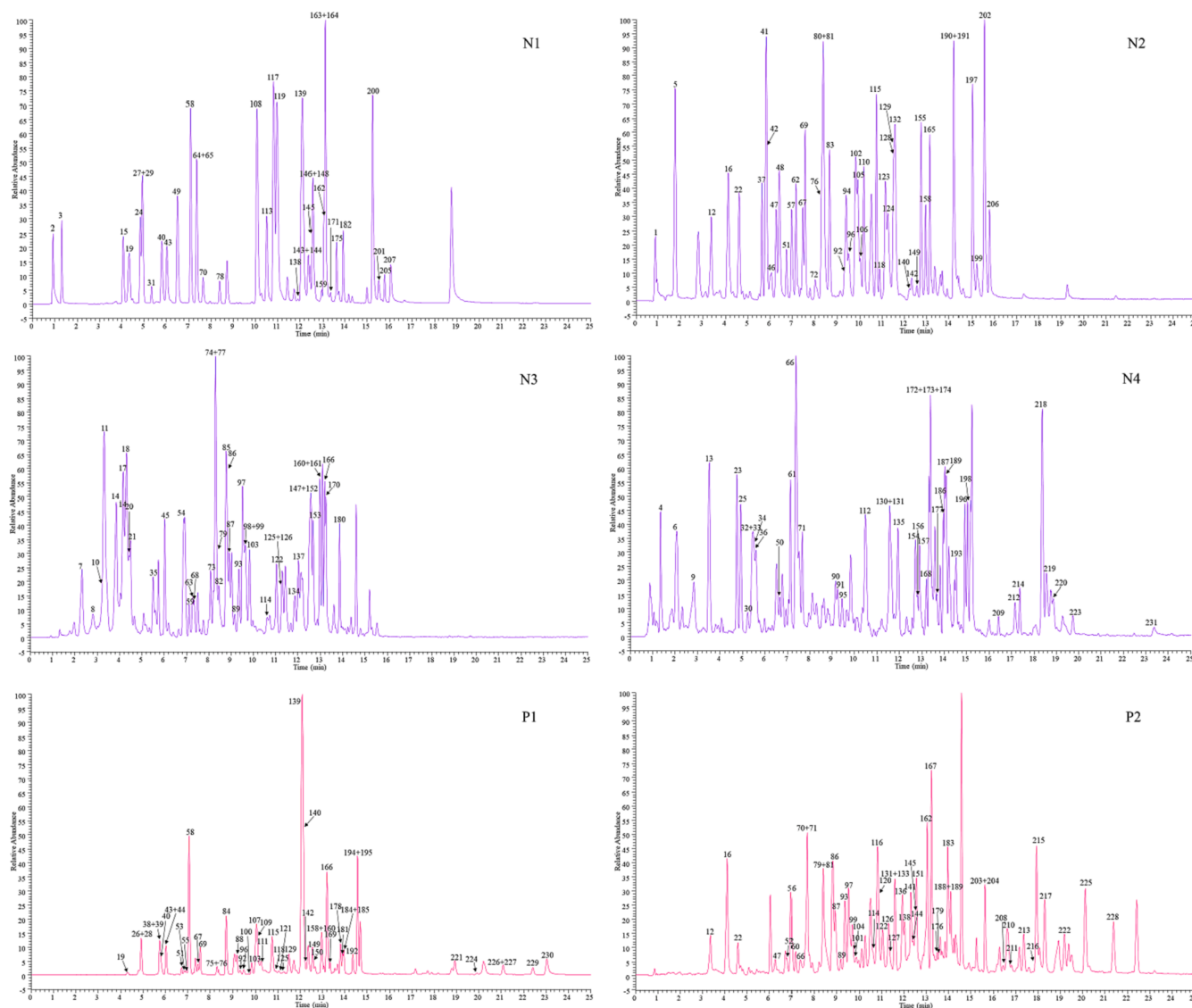


Fig. 2. The high resolution extracted ion chromatograms (HREICs) of QKDG in the positive (P) and negative ion modes (N). N1 m/z 179.03498, 191.01972, 299.05611, 315.05102, 353.08780, 359.07724, 375.12967, 403.12458, 415.10345, 435.15079, 461.10893, 461.16644, 507.11441, 515.11949, 519.18718, 535.16684, 579.20831, 609.14610, 623.19814, 719.16175; N2: m/z 177.01933, 191.05611, 253.07176, 269.04554, 285.04046, 301.03537, 329.06667, 361.11402, 367.10345, 373.11402, 387.16605, 389.10893, 431.09837, 449.14532, 461.07254, 473.07254, 477.10384, 477.14023, 491.11949, 515.14063, 547.14571, 593.15119, 609.18249, 637.10463; N3: m/z 197.04554, 239.09249, 283.15509, 311.04085, 315.07215, 335.13475, 341.08781, 357.13436, 445.07763, 445.11402, 447.09328, 447.15079, 463.08819, 481.09876, 505.15627, 507.17192, 521.13006, 563.14062, 607.20322, 621.18249, 623.16175, 639.19305, 717.14610; N4: m/z 169.01424, 207.06628, 223.09758, 267.06628, 271.06119, 283.06119, 295.04594, 299.11362, 327.05102, 329.08780, 331.06706, 337.09289, 339.07215, 344.04015, 349.08636, 355.10345, 373.09289, 373.12927, 387.14492, 407.09837, 433.11402, 435.12967, 453.14023, 467.21339, 473.14532, 477.06746, 503.17701, 504.18751, 519.15079, 535.18209, 579.17192, 653.17232, 677.15119, 709.19853, 729.26113, 755.24040, 769.25605, 825.46419, 867.47475; P1: m/z 187.08658, 193.04953, 239.08150, 249.14852, 255.06518, 287.09140, 301.10705, 305.10196, 317.10196, 327.13393, 335.11252, 345.09687, 355.10235, 359.11252, 389.12309, 417.11800, 433.11292, 447.09218, 459.12857, 463.12348, 479.11840, 523.14461, 538.22828, 549.16026, 579.17083, 595.16574, 607.20213, 625.17631; P2: m/z 187.03897, 191.10665, 203.03388, 217.04953, 223.06009, 233.04444, 247.06009, 247.09648, 249.06585, 263.08150, 267.07640, 271.09648, 277.10705, 279.07641, 319.11761, 339.10744, 342.16998, 359.07614, 369.11800, 431.13365, 449.10783, 461.14422, 465.10275, 503.11840, 517.13405, 517.15518, 565.15518, 627.15557, 655.18687, 707.25215.

sugar moiety reduced to produce a distinct fragment ion at $[Y]^-$ ion in O-glycosidic flavonoid compounds (Zhang et al., 2017). Furthermore, it is helpful in determining the presence of special functional groups in the structures in which the neutral loss of a molecule of H_2O (18.011 Da), CO (27.995 Da), or CO_2 (43.990 Da) and the cleavage of hexose occurred in the C-glycosidic flavonoid (Li et al., 2015). Peak 69 produced precursor ion $[M-H]^-$ at m/z 547.14571 ($C_{26}H_{27}O_{13}^-$), which produced the fragment ions at m/z 325.0700 $[M-H-132.0417-90.0311]^-$, thus indicating the neutral elimination of the pentose moiety and characteristic cleavage of the 0/3 bond, 295.0609 $[M-H-132.0417-120.0417]^-$ by the loss of pentose moiety and cleavage of the 0/2 bond. Subsequently, an ion was

obtained at m/z 267.0660 by the neutral loss of CO from m/z 295.060 in ESI⁻ mode. Peak 69 also yielded a precursor ion $[M+H]^+$ at m/z 549.16026 ($C_{26}H_{29}O_{13}^+$), which was fragmented into m/z 417.1164, corresponding to $[M+H-132.0417]^+$, by the cleavage of pentose, m/z 297.0745 $[M+H-132.0417-120.0417]^+$, m/z 399.1058 $[M+H-132.0417-18.0100]^+$, and m/z 381.0953 $[M+H-132.042-36.022]^+$ owing to the loss of one H_2O and two H_2O from m/z 417.1164, and m/z 351.0848 $[M+H-C_5H_8O_4-2H_2O-OCH_2]^+$ in ESI⁺ mode. Compared with the reference substance, peak 69 was identified as puerarin apioside. Peak 139 produced a precursor ion $[M-H]^-$ at m/z 461.10893 ($C_{26}H_{27}O_{13}^-$), which yielded fragment ions at m/z 299.0555 $[M-H-C_6H_{10}O_5]^-$,

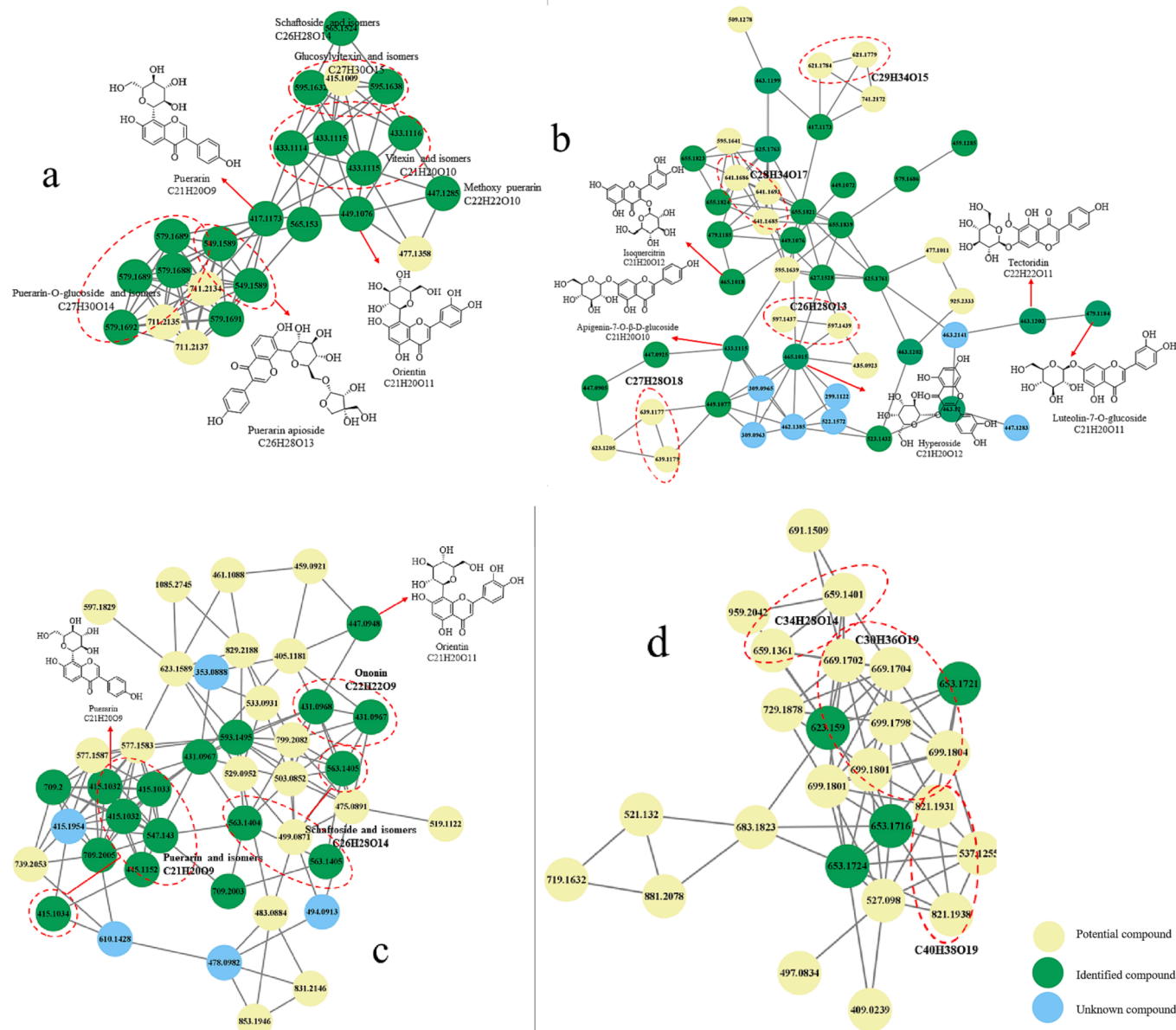


Fig. 3. The Feature-based molecular network of flavonoids of QQKDG extract in positive ion mode (a,b) and negative ion mode (c,d). a,c isoflavones; b,d flavones.

284.0318 $[M-H-C_6H_{10}O_5-CH_3]^-$, 283.0246 $[M-H-C_6H_{10}O_5-CH_4]^-$, 256.0335 $[M-H-C_6H_{10}O_5-CH_3-CO]^-$, and 240.0422 $[M-H-C_6H_{10}O_5-CH_3-CO_2]^-$. Peak 139 also exhibited an $[M+H]^+$ ion at m/z 463.12348, along with MS^2 fragments at m/z 301.0695 $[M+H-C_6H_{10}O_5]^+$ and 286.0458 $[M+H-C_6H_{10}O_5-CH_3]^+$. Based on the mass of MS fragmentation and standards, this compound was identified as tectoridin. The $[M-H]^-$ ions of flavones, flavonols, flavanones, and dihydrochalcones underwent a neutral loss of CH_3 , CO , CO_2 , and H_2O , along with a Retro-Diels-Alder (RDA) fragmentation reaction (Liu et al., 2005). Peak 99 generated a precursor ion $[M-H]^-$ at m/z 447.09328 ($C_{21}H_{19}O_{11}$), and was fragmented into m/z 285.0402 $[M-H-162.0523]^-$ by the loss of the $C_6H_{10}O_5$ at the C-7 position, and into 151.0025 $[C_7H_3O_4]^-$ and 133.0283 $[C_8H_5O_2]^-$ by RDA cleavage. Thus, it was unambiguously characterized as luteolin-7-O-glucoside by comparing its retention time and fragment ions with the reference standard. The proposed fragmentation pathways for puerarin apioside, tectoridin, and luteolin-7-O-glucoside were shown in Fig. 4a, b, c, respectively.

3.2.2. Identification of phenylethanoid glycosides

Reportedly, the common chemical structures of phenylethanoid glycosides are composed of saccharides (including rhamnose, glucose, and phenethyl alcohol (C_6-C_2) moieties) and linked aromatic acids (including caffeic acid, coumaric acid, and ferulic acid) via glycosidic bonds (Zheng et al., 2014; Wang et al., 2019). Phenylethanoid glycosides, detected in QQKDG, are a type of signature ingredient and the main components that play therapeutic effects; they are rooted in *Forsythia suspensa* (Shao et al., 2017). Furthermore, phenylethanoid glycosides can regulate various signaling pathways to play an anti-inflammatory role, and are promising as a supplement for anti-inflammatory drugs. In the ESI⁺ mode, the primary and representative phenylethanoid glycosides lost were glucose (Glu $C_6H_{10}O_5$, 162.0523 Da), rhamnose (Rha $C_6H_{10}O_4$, 146.0574 Da), H_2O (18.0101 Da), CO (27.9943 Da), and CO_2 (43.9893 Da). In addition, a series of lower-molecular-weight aromatic acids showed regular fragmentation patterns. For instance, caffeic acid ($C_9H_7O_4$, m/z 179.0339) produced ions at m/z 135.0441 ($C_8H_7O_2^-$) and 161.02333 ($C_9H_5O_3^-$) by the further loss of CO_2 and H_2O ; ferulic acid ($C_{10}H_9O_4$, m/z 193.0495) yielded an ion at

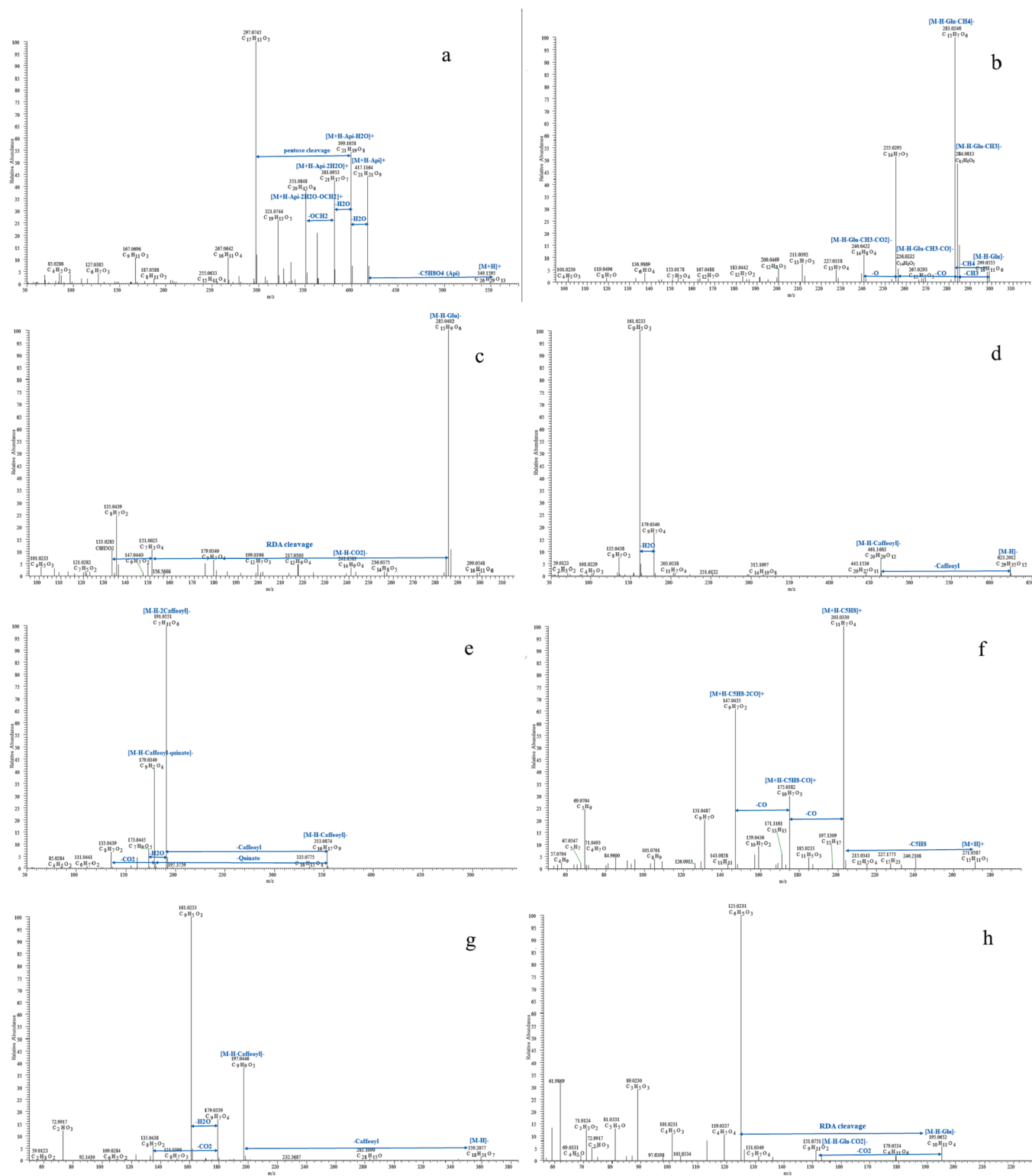


Fig. 4. The proposed fragmentation pathways of chemicals of QKGD in positive and negative modes, a, puerarin apioside; b, tectoridin; c, luteolin-7-O-glucoside; d, forsythoside A; e, isochlorogenic acid A; f, isomeratorin; g, rosmarinic acid; h, sweroside; i, magnoflorine.

m/z 175.0390 ($C_{10}H_7O_3^-$) by the loss of H₂O; and coumaric acid ($C_9H_7O_3^-$, m/z 163.0390) generated ions at m/z 145.0284 ($C_9H_5O_2^-$) and 119.0491 ($C_8H_7O^-$) by the further loss of H₂O and CO₂, respectively. In this study, the FBMN contained a total of 91 nodes, of which numerous were phenylethanoid glycosides according to their fragment ions (Fig. 5); however, only a few nodes were analyzed and identified.

Peaks 108, 117, 119, and 146, eluted at 10.05, 10.80, 10.95, and 12.54 min, respectively, showed the same precursor ion $[M-H]^-$ at m/z 623.19814 ($C_{29}H_{35}O_{15}^-$), and exhibited similar fragment ions at m/z 461.1665 [$M-H-C_6H_{10}O_5^-$], 179.0340 [caffeic acid-H]⁻, and 161.0233 [caffeic acid-H₂O]⁻. Peaks 117 and 119 were confirmed to be forsythoside. Additionally, peaks 108 and 146 were tentatively identified

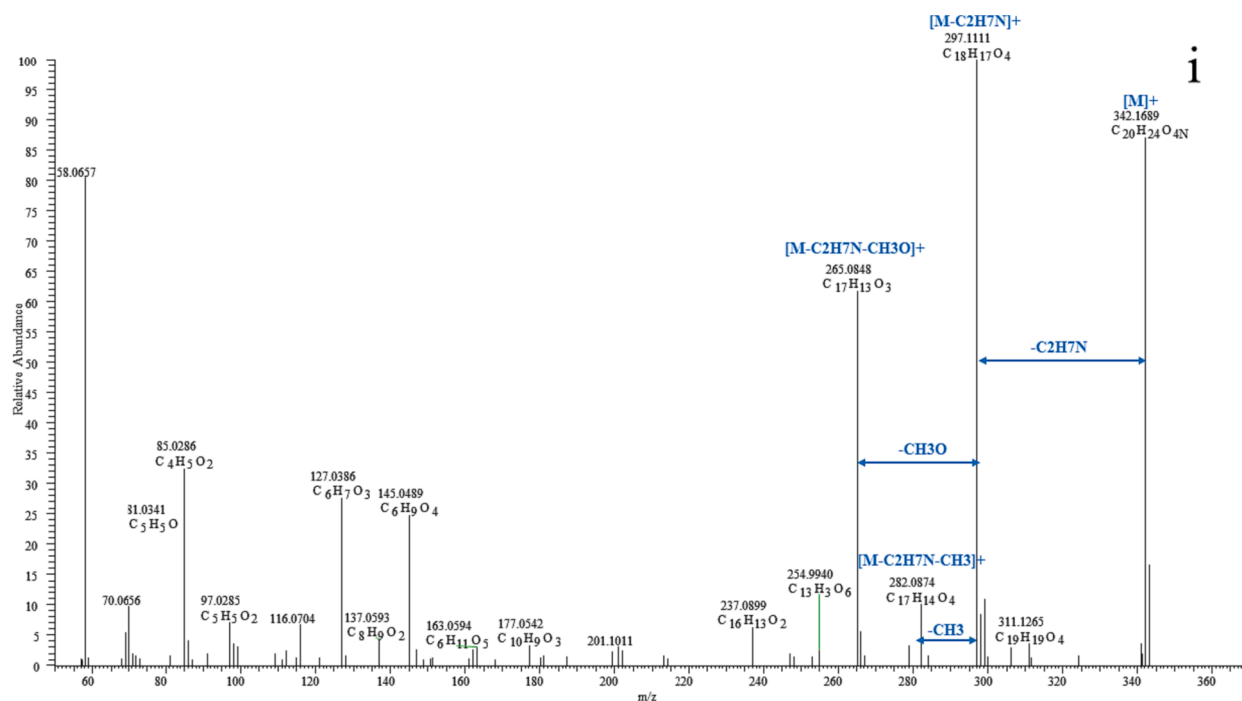


Fig. 4. (continued).

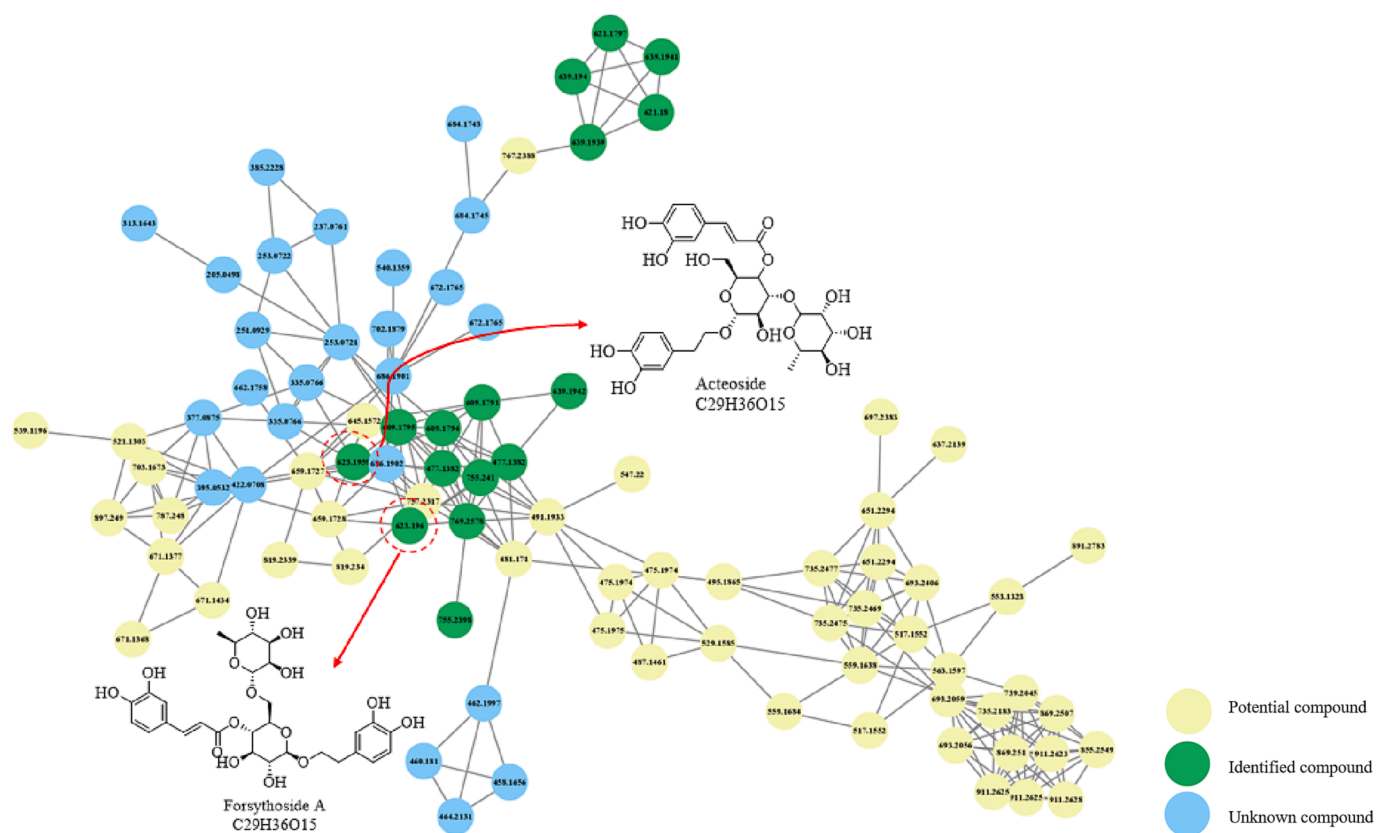


Fig. 5. The Feature-based molecular network of phenylethanoid glycosides of QKDG extract in negative ion mode.

as forsythoside H and I, respectively, based on their retention behavior on a reversed-phase chromatographic column and similar fragmentation patterns (Sun et al., 2015). Peaks 106 and 132 (Rt 10.02 and 11.58 min, respectively) were assigned to calceolariosides A and B in the FBMN. The proposed fragmentation pathway of forsythoside A is shown in

Fig. 4d.

3.2.3. Identification of chlorogenic acid derivatives

Chlorogenic acids (CGAs) are a group of esters of hydroxycinnamic acids (HCAs), which include caffeic acid (CA), ferulic acid (FA), p-

coumaric acid (p-CoA), and quinic acid (QA), which yield caffeoylquinic acid (CQA), feruloylquinic acid (FQA), and p-coumaroylquinic acid (pCoQA), respectively; additionally, the majority of CGAs were mono- and di-caffeoylquinic acids (CQAs) (Ramabulana et al., 2020). These compounds exist predominantly in several plants, which possess some notable pharmacological properties, such as anti-inflammatory and antioxidant properties, and contribute significantly to the total dietary intake of phenols (Marques and Farah, 2009). The caffeic acid (m/z 179.0338 $C_9H_7O_4$), ferulic acid (m/z 193.0495 $C_{10}H_9O_4$), and p-coumaric acid (m/z 163.0390 $C_9H_7O_3$) are the common types of hydroxycinnamic acids, which generate a series of characteristic fragment ions at m/z 135.0441 ($C_8H_7O_2$) and 161.0233 ($C_9H_5O_3$) by the further loss of CO_2 and H_2O from m/z 179.0338 ($C_9H_7O_4$); m/z 178.0261 ($C_9H_6O_4$), 149.0597 ($C_9H_9O_2$), and 134.0362 ($C_8H_6O_2$) by the further loss of CH_3 , CO_2 , CO_2H_2O from m/z 193.0495 ($C_{10}H_9O_4$), respectively; and 119.0491 (C_8H_7O) by the loss of CO_2 from m/z 163.0390. Meanwhile, the fragment ions at m/z 173.0444 ($C_7H_9O_5$), 127.0389 ($C_6H_7O_3$), and 111.0440 ($C_6H_7O_2$), by the loss of H_2O , $2H_2OCO$, and $2H_2OCO_2$ from m/z 11.0550 ($C_7H_{11}O_6$), respectively, were characteristic ions of quinic acid in the ESI⁻ mode. In this study, the FBMN contained 28 nodes in the positive ion mode and 21 nodes in the negative ion mode in connection with CGAs; additionally, most of the nodes were hydroxycinnamylquinic acids and dihydroxycinnamylquinic acids (Fig. 6). Peaks **70**, **138**, **144**, **145**, and **162**, eluted at 7.63, 12.05, 12.39, 12.52, and 13.04 min, respectively, exhibited the same precursor ion $[M-H]^-$ at m/z 515.11949 ($C_{25}H_{23}O_{12}$), which produced fragment ions at m/z 353.0874 $[M-H-C_9H_6O_3]^-$ by the loss of a caffeoyl residue, 179.0340 [caffeic acid-H]⁻, 135.0439 [caffeic acid-H-CO₂]⁻, 191.0552 [quinic acid-H]⁻, and 173.0445 [quinic acid-H-H₂O]⁻. Peaks **70**, **144**, **145**, and **162** were explicitly identified as 1,3-Dicaffeoylquinic acid, isochlorogenic acid B, isochlorogenic acid A, and isochlorogenic acid C, respectively, by comparison with corresponding reference standards. Peak **138** as its isomer had a similar precursor ion and fragmentation patterns and was tentatively identified as 1, 4-Dicaffeoylquinic acid according to its chromatographic retention behavior. The proposed fragmentation pathway of isochlorogenic acid A is shown in Fig. 4e.

3.2.4. Identification of coumarins

Coumarins are common lactones formed by the intramolecular dehydration of *cis*- α -hydroxycinnamic acid and are characterized by a benzene ring attached to an α -pyrone ring. Coumarins are the most abundant components of *Angelicae dahuricae* (AD) in QKDG and possess various pharmacological activities, including antioxidant, anticancer, and anticoagulant effects (Lu et al., 2020). The coumarins separated from AD are predominantly linear furocoumarins, which consist of a simple coumarin as the parent nucleus and a substituent group at the seven and six positions. Furthermore, the positions of the benzene rings of simple coumarins at the five, six, seven, and eight sites were replaced by hydroxyl, methoxyl, methylenedioxy, and isopentenyl groups (Zhu and Jiang, 2018). In ESI⁺ mode, the primary and representative losses of H_2O (18.0100 Da), CH_3 (15.0229 Da), CO (27.9943 Da), and CO_2 (43.9893 Da) occurred in simple coumarins. In this study, FBMN contained 31 nodes, of which 22 were identified as coumarins and 5 were regarded as potential compounds according to their MS² fragment ions (Fig. 7). Peak **195** showed a precursor ion $[M+H]^+$ at m/z 317.10196 ($C_{17}H_{17}O_6^+$), which yielded product ions at m/z 233.0435 $[M+H-C_5H_8O]^+$, 231.0279 $[M+H-C_5H_{10}O]^+$, 218.0202 $[M+H-C_5H_8O-CH_3]^+$, 203.0332 $[M+H-C_5H_{10}O-CO]^+$, and 175.0383 $[M+H-C_5H_{10}O-2CO]^+$. Therefore, peak **195** was confirmed to be byakangelicol based on a retention time and fragmentation pathway similar to that of the reference standards. Peak **228** displayed the parent ion $[M+H]^+$ at m/z 271.09648 ($C_{16}H_{14}O_4^+$), thus indicating the presence of characteristic fragment ions at m/z 203.0330 $[M+H-C_5H_8]^+$, 175.0382 $[M+H-C_5H_8-CO]^+$, and 147.0435 $[M+H-C_5H_8-2CO]^+$. Thus, it was unambiguously identified as isoimperatorin by comparing the retention time and parent and fragment ions with those of the standard. Peaks **185** and

192 both showed quasi-molecular ion $[M+H]^+$ at m/z 305.10196 ($C_{16}H_{17}O_6^+$) and produced a series of similar characteristic fragment ions at m/z 203.0330 $[M+H-C_5H_{10}O_2]^+$, 175.0383 $[M+H-C_5H_{10}O_2-CO]^+$, and 147.0434 $[M+H-C_5H_{10}O_2-2CO]^+$, which were tentatively characterized as prangenin hydrate, oxypeucedan hydrate, respectively, based on their different retention times in the HPLC chromatogram. The proposed fragmentation pathway of isoimperatorin is shown in Fig. 4f.

3.2.5. Identification of phenolic acids

Phenolic acids are a class of common compounds formed by the substitution of hydrogen atoms on benzene rings with carboxylic acid ($-COOH$) and hydroxyl groups ($-OH$), and are widely present in plants, plant foods, and human metabolites. Phenolic acids are excellent antioxidants that can alleviate physical damage and chronic diseases caused by free radicals (Chen et al., 2020). In this study, 36 phenolic acids were identified in QKDG. However, no related FBMN cluster of phenolic acids was built in the GNPS, most likely because phenolic acids contain numerous varieties such as caffeic acid, gallic acid, protocatechuic acid, and ferulic acid, and no correlation exists between the secondary fragment ions of these compounds. Peak **164** exhibited a quasi-molecular ion $[M-H]^-$ at m/z 359.07724 ($C_{18}H_{15}O_6$), which produced the characteristic fragment ions at m/z 197.0446 $[M-H-C_9H_6O_3]^-$ by the loss of the caffeoyl group, 179.0339 $[M-H-C_9H_6O_3-H_2O]^-$, and 161.0233 $[M-H-C_9H_6O_3-2H_2O]^-$, as shown in Fig. 8. Therefore, peak **164** was accurately identified as rosmarinic acid based on chromatographic information and fragmentation patterns of the reference substance. Peaks **6** and **49** were identified as gallic and caffeic acids, respectively. Peak **9** presented a $[M-H]^-$ ion at m/z 331.06706 ($C_{13}H_{15}O_{10}$), corresponding to gallic acid linked to a glucose, fragment ions at m/z 169.0112 $[M-H-162.0522]^-$ from gallic acid and m/z 125.0231 $[M-H-162.0522-43.9893]^-$ corresponding to the loss of CO_2 ; hence, peak **9** was tentatively identified as gallic acid-4-O-glucoside. Peaks **21** and **35** displayed the precursor ion $[M-H]^-$ at m/z 341.08781 ($C_{15}H_{17}O_6$), which yielded fragment ions at m/z 179.03440 $[M-H-C_6H_{10}O_5]^-$ and 135.0439 $[M-H-C_6H_{10}O_5-CO_2]^-$ by the subsequent loss of CO_2 . Thus, they were tentatively characterized as caffeic acid-O-glucosides. Peak **83** showed a precursor ion $[M-H]^-$ at m/z 449.14532 ($C_{22}H_{25}O_{10}$) and then yielded product ions at m/z 315.1093 $[M-H-C_8H_6O_2]^-$, 193.0498 ($C_{10}H_9O_4$), 175.0390 $[C_{10}H_9O_4-H_2O]^-$, and 165.0547 $[C_{10}H_9O_4-CO]^-$. According to the fragmentation patterns reported in the literature (Sun et al., 2015), peak **83** was tentatively identified as forsythenside F. The proposed fragmentation pathway of rosmarinic acid is shown in Fig. 4g.

3.2.6. Identification of terpenoids and alkaloids

In this study, 14 terpenoids, including 10 monoterpenes, 2 sesquiterpenes, and 2 triterpenes, were identified according to the chromatographic retention behavior and fragmentation patterns of the in-house library. Peak **64** displayed a precursor ion $[M+HCOOH-H]^-$ at m/z 403.12458 ($C_{17}H_{23}O_{11}$), which generated the aglycone ion $[M-H-C_6H_{10}O_5]^-$ at m/z 195.065 ($C_{10}H_{11}O_4$) by the neutral loss of a glucose; the subsequent loss of CO_2 further produced the fragment ion $[M-H-C_6H_{10}O_5-CO_2]^-$ at m/z 151.0751 ($C_9H_{11}O_2$), and 125.0231 ($C_6H_5O_3$) originated from the RDA cleavage. Thus, it was identified as a sweroside by comparing the retention time and fragmentation pathways with those of the reference compound. Peaks **15**, **29**, and **31** all displayed the deprotonated molecular ion $[M-H]^-$ at m/z 375.12967 ($C_{16}H_{23}O_{10}$), and produced similar MS/MS spectrum patterns. They produced several fragment ions at m/z 213.0761 $[M-H-C_6H_{10}O_5]^-$, 169.0859 $[M-H-C_6H_{10}O_5-CO_2]^-$, 151.0753 $[M-H-C_6H_{10}O_5-CO_2-H_2O]^-$, and 125.0595 ($C_7H_9O_2$), which were tentatively identified as 8-epiloganic acid (peak **15**), loganic acid (peak **29**), and adoxosidic acid (peak **21**), according to the elution order on the chromatographic column and fragment pathways (He et al., 2020). Additionally, a total of 10 alkaloids that mainly originated from *Isatis Tinctoria* and *Folium Isatidis* in QKDG were detected and characterized. Peak **56** was assigned to magnoflorine by comparing its retention time and MS²

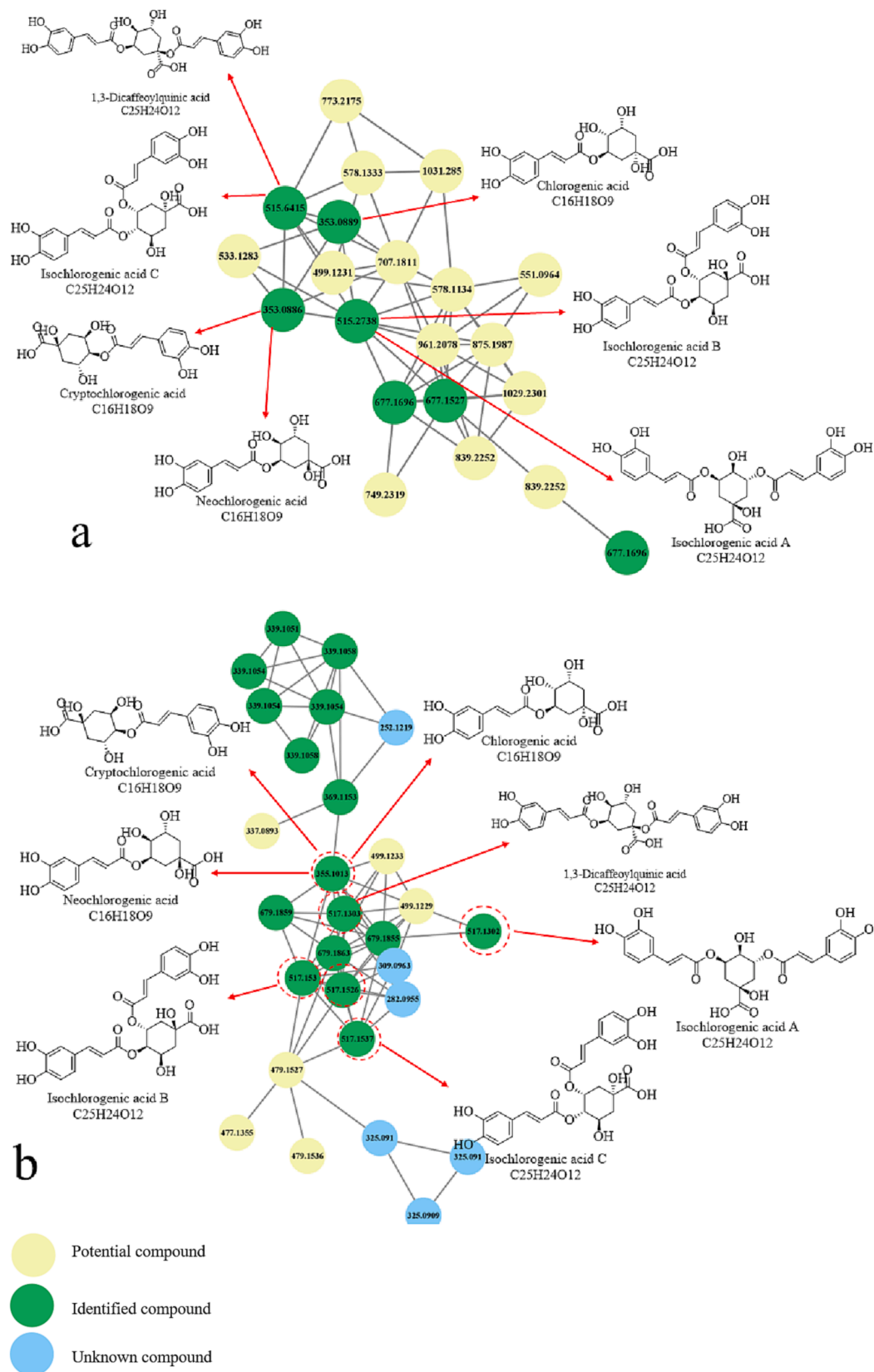


Fig. 6. The Feature-based molecular network of chlorogenic acid derivatives of QQKDG extract in positive (a) and negative (b) ion modes.

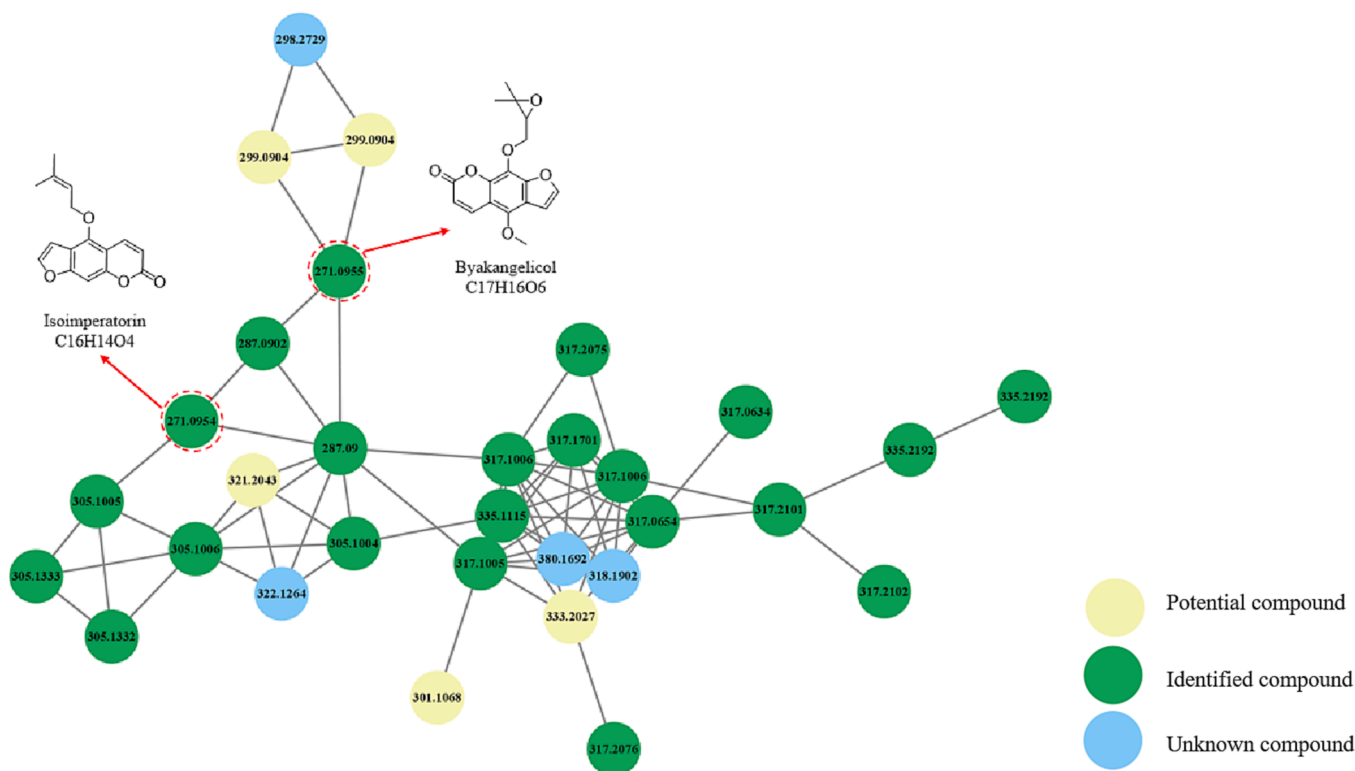


Fig. 7. The Feature-based molecular network of coumarins of QKDG extract in positive ion mode.

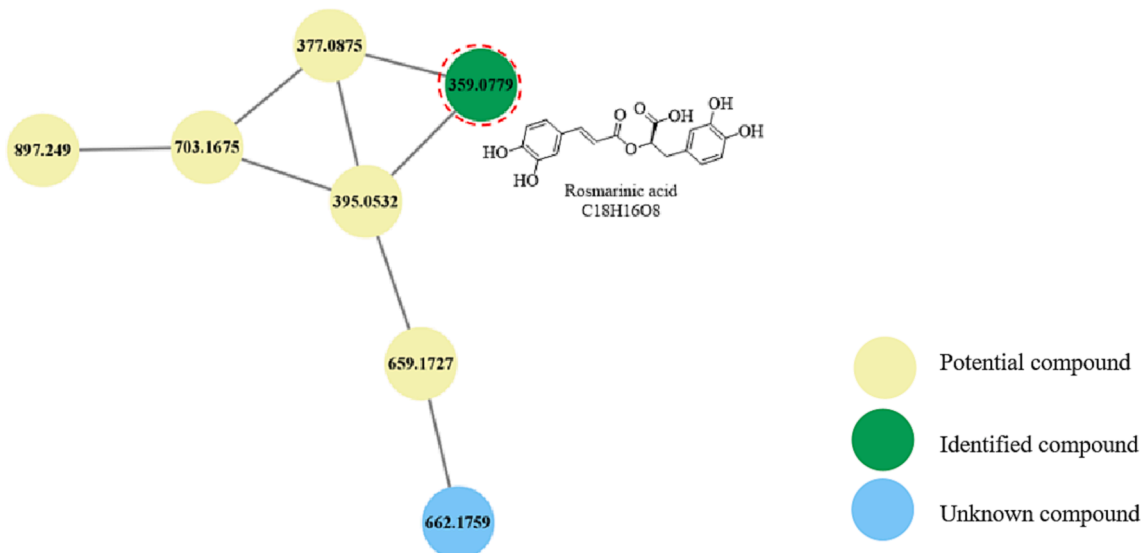


Fig. 8. The Feature-based molecular network of rosmarinic acid derivatives of QKDG extract in negative ion mode.

spectrum with those of the reference compound. Peaks 222 and 225 showed a $[M + H]^+$ ion at m/z 263.08150 ($C_{16}H_{11}N_2O_2^+$), which produced fragment ions at m/z 235.0856 $[M + H - CO]^+$ and 219.0907 $[M + H - CO_2]^+$, which were tentatively characterized as indigo and indirubin, respectively, according to the retention time and fragmentation patterns in the literature (Yan et al., 2017). The proposed fragmentation pathways for sweroside and magnoflorine are shown in Fig. 4h and i.

3.2.7. Identification of lignans and other compounds

Lignans are a class of natural products derived from the oxidative coupling of two C_6-C_3 units that can combine with sugar groups to form glycosides. Lignans have been used in traditional medicine for the

treatment of diseases for a long time owing to their biological activities, including antioxidant, antitumor, anti-inflammatory (Teponno et al., 2016). In this study, 10 lignans were characterized using an in-house library and GNPS (Fig. 9). Peaks 148 and 171 both showed a quasi-molecular ion peak $[M - H]^-$ at m/z 519.18718 ($C_{26}H_{31}O_{11}^-$) and produced a similar fragment ion at m/z 357.1342 ($C_{20}H_{21}O_6^-$), corresponding to $[M - H - C_6H_{10}O_5]^-$, due to the loss of a glucose group. Hence, peaks 148 and 171 were tentatively characterized as pinoresinol-O-glucoside and matairesinoside, respectively, according to the elution order of the chromatographic column and fragment pathways (He et al., 2020). Additionally, the other seven compounds, namely Cgmp, N-octanoylsucrose, 3-(2'-Hydroxyphenyl)-4-(3H)-

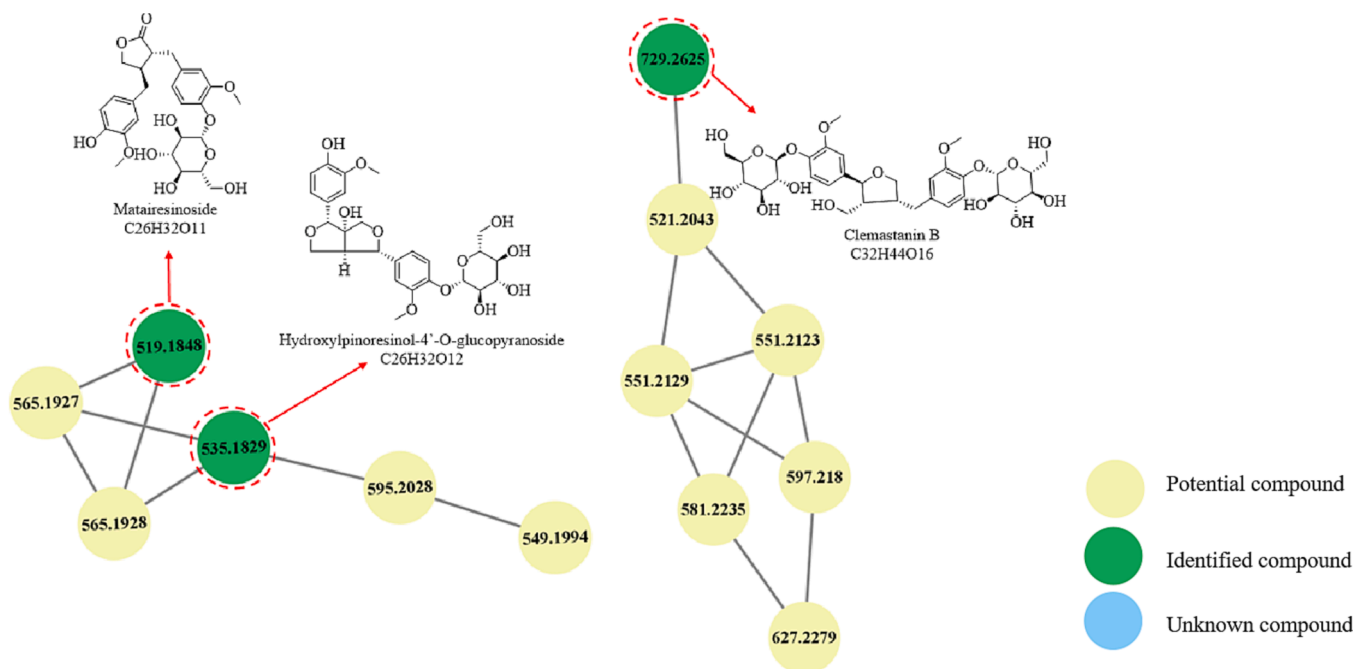


Fig. 9. The Feature-based molecular network of lignans of QQKDG extract in negative ion mode.

quinazolinone, ligustilide, Junipegenin C, pogostone, and kuzubutenolide A, were detected and putatively identified by matching the MS/MS product ions with in-house library. Peak 217 exhibited an $[M + H]^+$ ion at m/z 191.10665, which produced product ions at m/z 145.1012 ($C_{11}H_{13}$) owing to the loss of H_2O and CO , and 117.0699 (C_9H_9), derived from the ion at m/z 145.1012 through the elimination of 28.0305 (C_2H_4). It was identified as ligustilide by comparing the chromatographic behavior and MS/MS spectra with the reference standard.

4. Conclusion

In this study, an integrated strategy based on UHPLC-Q-Exactive-MS coupled with FBMN analysis was developed for systematical characterization of structural types and identification of chemical ingredients in the TCM prescription QQKDG. It is beneficial to exploring unknown or potential compounds, revealing the visualization of the structural relationships among molecules, and improving the efficiency of compounds identification using multiple databases matching and fragmentation patterns, which could effectively avoid the problems of high cost and low efficiency of natural products discovery in TCMs. Thus, a total of 231 compounds were accurately or tentatively characterized, among which 224 compounds including cclavonoids, phenolic acids, phenylethanoid glycosides, coumarins, chlorogenic acids, terpenoids, alkaloids, and lignans were identified for the first time. Moreover, numerous unassigned clusters and nodes were observed in the GNPS, which is conducive to the discovery of novel compounds. However, the results revealed that FBMN did not benefit the further characterization of isomers with high confidence, and distinguishing isomers is challenging at present. In summary, this systematic study on QQKDG provides a convenient and powerful analytical strategy for the rapid screening and detection of the chemical constituents of TCM formulas. The results of this study provide a theoretical basis for quality control and promote the development of modern QQKDG prescription.

Funding

This study was funded by the Science and Technology Innovation Program of Hunan Province (no. 2022RC1228), Hunan Province Social Science Innovation Research Base (Ethnic medicine and ethnic culture

research base), Research Project of Sichuan Provincial Administration of Traditional Chinese Medicine (2021MS220) and Research Project of Hospital of Chengdu University of Traditional Chinese Medicine (20ZJ18).

Declaration of competing interest

The authors declare that they have no known competing financial interests or personal relationships that could have appeared to influence the work reported in this paper.

Appendix A. Supplementary material

Supplementary data to this article can be found online at <https://doi.org/10.1016/j.arabjc.2023.105463>.

References

- Aravilli, R.K., Vikram, S.L., Kohila, V., 2017. Phytochemicals as potential antidotes for targeting NF- κ B in rheumatoid arthritis. *3 Biotech.* 7, 1–11.
- Chen, J., Yang, J., Ma, L., Li, J., Shahzad, N., Kim, C.K., 2020. Structure-antioxidant activity relationship of methoxy, phenolic hydroxyl, and carboxylic acid groups of phenolic acids. *Sci. Rep.* 10 (1), 2611.
- Chen, L., Yao, C., Li, J., Wang, J., Yao, S., Shen, S., 2021. Systematic characterization of chemical constituents in Mahuang decoction by UHPLC tandem linear ion trap-Orbitrap mass spectrometry coupled with feature-based molecular networking. *J. Sep. Sci.* 44 (14), 2717–2727.
- Choi, S., Woo, J.-K., Jang, Y.-S., Kang, J.-H., Jang, J.-E., Yi, T.-H., 2016. Fermented Pueraria Lobata extract ameliorates dextran sulfate sodium-induced colitis by reducing pro-inflammatory cytokines and recovering intestinal barrier function. *Lab Anim.* 32, 151–159.
- Corradini, E., Foglia, P., Giansanti, P., Gubbiotti, R., Samperi, R., Lagana, A., 2011. Flavonoids: chemical properties and analytical methodologies of identification and quantitation in foods and plants. *Nat. Prod. Res.* 25 (5), 469–495.
- Dias, M.C., Pinto, D.C., Silva, A.M., 2021. Plant flavonoids: chemical characteristics and biological activity. *Molecules.* 26 (17), 5377.
- Fu, S., Cheng, R., Deng, Z., Liu, T., 2021. Qualitative analysis of chemical components in Lianhua Qingwen capsule by HPLC-Q Exactive-Orbitrap-MS coupled with GC-MS. *J. Pharm. Sci.* 11 (6), 709–716. <https://doi.org/10.1016/j.jpha.2021.01.004>.
- Gao, W.-Y., Si, N., Li, M.-L., Gu, X.-R., Zhang, Y., Zhou, Y.-Y., 2021. The integrated study on the chemical profiling and in vivo course to explore the bioactive constituents and potential targets of Chinese classical formula Qingxin Lianzi Yin Decoction by UHPLC-MS and network pharmacology approaches. *J. Ethnopharmacol.* 272, 113917.
- Harborne, J.B., 2013. The flavonoids: advances in research since 1980.

- He, H.-H., Yao, J.-B., Chang, W.-Q., Wang, J.-F., Ying, K., Luo, T.-T., 2020. Analysis of Chemical Material Basis of Compound Yuxingcao Mixture Based on HPLC-LTO Orbitrap MS/MS Technology. *Asia-Pacific Tradit. Med.* 16 (08), 37–44.
- Hu, R.-F., Sun, X.-B., 2017. Design of new traditional Chinese medicine herbal formulae for treatment of type 2 diabetes mellitus based on network pharmacology. *Chin. J. Nat. Med.* 15 (6), 436–441.
- Karak, P., 2019. Biological activities of flavonoids: an overview. *J. Pharm. Sci. Res.* 10 (4), 1567–1574.
- Li, Y., Cui, Z., Li, Y., Gao, J., Tao, R., Li, J., 2022. Integrated molecular networking strategy enhance the accuracy and visualization of components identification: a case study of Ginkgo biloba leaf extract. *J. Pharm. Biomed. Anal.* 209, 114523.
- Li, B., Li, L., Zhao, A., Han, B., Fan, Y., Liu, C., 2015. Preparative separation of isoflavones in plant extract of Pueraria lobata by high performance counter-current chromatography. *J. Anal. Methods* 7 (4), 1321–1327.
- Liu, R., Ye, M., Guo, H., Bi, K., Guo, D.a., 2005. Liquid chromatography/electrospray ionization mass spectrometry for the characterization of twenty-three flavonoids in the extract of Dalbergia odorifera. *Rapid Commun. Mass Spectrom.* 19 (11), 1557–1565.
- Lu, Y., Wu, H., Yu, X., Zhang, X., Luo, H., Tang, L., 2020. Traditional Chinese Medicine of Angelicae Pubescentis Radix: a Review of Phytochemistry. *Pharmacol. Pharmacokinetics. Front. Pharmacol.* 11 <https://doi.org/10.3389/fphar.2020.00335>.
- Marques, V., Farah, A., 2009. Chlorogenic acids and related compounds in medicinal plants and infusions. *Food Chem.* 113 (4), 1370–1376.
- Pang, B., Zhu, Y., Lu, L., Gu, F., Chen, H., 2016. The applications and features of liquid chromatography-mass spectrometry in the analysis of traditional Chinese medicine. *Evid. Based Complement. Altern. Med.*
- Qu, B., Liu, Y., Shen, A., Guo, Z., Yu, L., Liu, D., 2023. Combining multidimensional chromatography-mass spectrometry and feature-based molecular networking methods for the systematic characterization of compounds in the supercritical fluid extract of Tripterygium wilfordii Hook F. *Analyst* 148 (1), 61–73.
- Ramabulana, A.-T., Steenkamp, P., Madala, N., Dubery, I.A., 2020. Profiling of chlorogenic acids from Bidens pilosa and differentiation of closely related positional isomers with the aid of UHPLC-QTOF-MS/MS-based in-source collision-induced dissociation. *Metabolites* 10 (5), 178.
- Shao, S.-Y., Feng, Z.-M., Yang, Y.-N., Jiang, J.-S., Zhang, P.-C., 2017. Forsythenosides A and B: two new phenylethanoid glycosides with a 15-membered ring from Forsythia suspensa. *Org. Biomol. Chem.* 15 (33), 7034–7039.
- Sun, H., Liu, M., Lin, Z., Jiang, H., Niu, Y., Wang, H., 2015. Comprehensive identification of 125 multifarious constituents in Shuang-huang-lian powder injection by HPLC-DAD-ESI-IT-TOF-MS. *J. Pharm. Biomed. Anal.* 115, 86–106.
- Teponno, R.B., Kusari, S., Spittler, M., 2016. Recent advances in research on lignans and neolignans. *Nat. Prod. Rep.* 33 (9), 1044–1092.
- Wang, X., Chang, X., Luo, X., Su, M., Xu, R., Chen, J., 2019. An integrated approach to characterize intestinal metabolites of four phenylethanoid glycosides and intestinal microbe-mediated antioxidant activity evaluation in vitro using UHPLC-Q-Exactive High-Resolution Mass Spectrometry and a 1, 1-Diphenyl-2-picrylhydrazyl-based assay. *Front. Pharmacol.* 10, 826.
- Wang, S., Chen, P., Jiang, W., Wu, L., Chen, L., Fan, X., 2014. Identification of the effective constituents for anti-inflammatory activity of Ju-Zhi-Jiang-Tang, an ancient traditional Chinese medicine formula. *J. Chromatogr. A.* 1348, 105–124.
- Wang, D., Fu, Z., Xing, Y., Tan, Y., Han, L., Yu, H., 2020. Rapid identification of chemical composition and metabolites of Pingxiao Capsule in vivo using molecular networking and untargeted data-dependent tandem mass spectrometry. *Biomed. Chromatogr.* 34 (9), e4882.
- Wang, N., Zhao, X., Li, Y., Cheng, C., Huai, J., Bi, K., 2018. Identification of the absorbed components and metabolites of modified Huo Luo Xiao Ling Dan in rat plasma by UHPLC-Q-TOF/MS/MS. *Biomed. Chromatogr.* 32 (6), e4195.
- Wozniak, D., Janda, B., Kapusta, I., Oleszek, W., Matkowski, A., 2010. Antimutagenic and anti-oxidant activities of isoflavonoids from Belamcanda chinensis (L.) DC. *Mutat. Res. Genet. Toxicol. Environ. Mutagen.* 696 (2), 148–153.
- Xia, L.-L., Wang, X.-H., Sheng, R., 2016. Simultaneous determination of seven constituents in Qingqiao Kangdu Granules by HPLC with switching wavelengths. *Chin. Hosp. Pharm. J. Dec.* 36 (23), 2065–2070. <https://doi.org/10.13286/j.cnki.chinhosp pharmacy.2016.23.07>.
- Xiong, G.-F., 2015. The Clinical Study of Randomized Double Blind and Parallel Control, which is to Compare the Efficacy between “Qingqiao Kangdu granules” Decocting-Free Granules and Traditional Decoction in the Treatment of Common Cold with Exogenous Wind-Heat Syndrome. *Chengdu Univ. Tradit. Chin. Med.*
- Xiong, G.-F., Ynag, T., Luo, Y., Ma, W.-Q., He, Y., 2014. Observation on the curative effect of Qingqiao Kangdu granules intelligent free decoction in treating cold with wind-heat syndrome. *Chin. J. Clin. Rational Drug Use* 7 (30), 111–112. <https://doi.org/10.15887/j.cnki.13-1389/r.2014.30.184>.
- Xu, H., Chen, K.-J., 2010. Herb-drug interaction: an emerging issue of integrative medicine. *Chinese J. Integrative Med.* 16, 195–196.
- Xu, J., Zhang, Y., 2020. Traditional Chinese medicine treatment of COVID-19. *Complement. Ther. Clin. Pract.* 39, 101165.
- Yan, J., Liu, S., Li, B.-P., Liu, Z.-Q., Guo, D.-F., 2017. Fingerprint Chromatograms and Chemical Components of Compound Indigowoad Root Granule by APCI-MS and LC-APCI-MSn. *J. Chin. Mass Spectrom. Soc.* 38 (03), 320–327.
- Yang, L., Yu, H., Hou, A., Man, W., Wang, S., Zhang, J., 2021. A review of the ethnopharmacology, phytochemistry, pharmacology, application, quality control, processing, toxicology, and pharmacokinetics of the dried rhizome of Atractylodes macrocephala. *Front. Pharmacol.* 12, 727154.
- Zhang, Z., Dong, Y., Huang, Y., Peng, L., 2015. Effect of total flavonoids from astragalus complanatus on paraquat poisoning-induced pulmonary fibrosis in rats and its mechanisms. *Chin J Ind. Hyg Occup. Dis.* 33 (11), 838–840.
- Zhang, Y., Lei, H., Tao, J., Yuan, W., Zhang, W., Ye, J., 2021. An integrated approach for structural characterization of Gui Ling Ji by traveling wave ion mobility mass spectrometry and molecular network. *RSC Adv.* 11 (26), 15546–15556.
- Zhang, F., Li, B., Wen, Y., Liu, Y., Liu, R., Liu, J., 2022. An integrated strategy for the comprehensive profiling of the chemical constituents of Aspongopus chinensis using UPLC-QTOF-MS combined with molecular networking. *Pharm Biol.* 60 (1), 1349–1364.
- Zhang, S., Zheng, Z.-P., Zeng, M.-M., He, Z.-Y., Tao, G.-J., Qin, F., 2017. A novel isoflavone profiling method based on UPLC-PDA-ESI-MS. *Food Chem.* 219, 40–47.
- Zheng, S., Jiang, X., Wu, L., Wang, Z., Huang, L., 2014. Chemical and genetic discrimination of Cistanches Herba based on UPLC-QTOF/MS and DNA barcoding. *PLoS One.* 9 (5), e98061.
- Zhu, J.J., Jiang, J.G., 2018. Pharmacological and nutritional effects of natural coumarins and their structure–activity relationships. *Mol. Nutr. Food Res.* 62 (14), 1701073.